Final Report March 1978

Shuttle Orbiter—IUS/DSP Satellite Interface Contamination Study

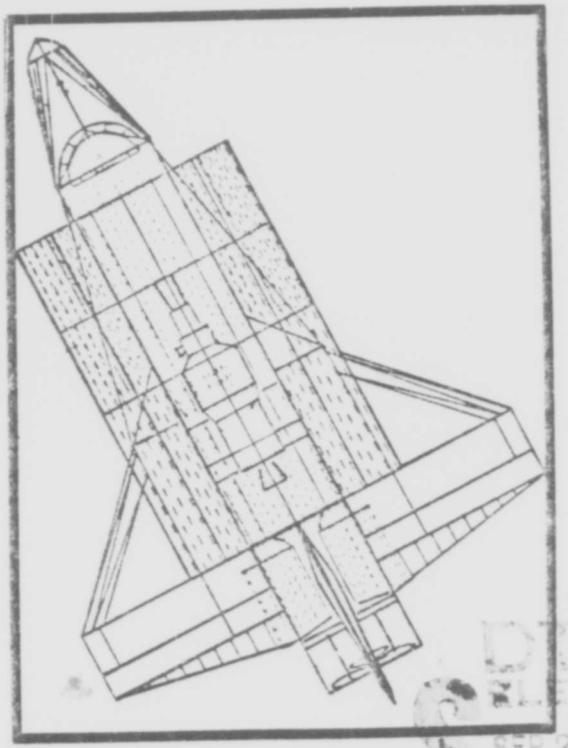

MARTIN MARIETTA

MCR-78-512
March 21, 1978

Technical Report

SHUTTLE ORBITER - IUS/DSP SATELLITE INTERFACE CONTAMINATION STUDY

FINAL REPORT

Contract NAS9-15335

RE: Contract F04701-77-C-0183
This is the correct contract number for Rept.
MCR-78-512
Per Lt. Dawn A. Adams, Space Division

Authors

R. O. Rantanen
D. A. Strange

Prepared for

Lyndon B. Johnson Space Center
Houston, Texas 77058

MARTIN MARIETTA AEROSPACE
Denver Division
P. O. Box 179
Denver, Colorado 80201

TABLE OF CONTENTS

Figures

TABLE OF CONTENTS (cont.)

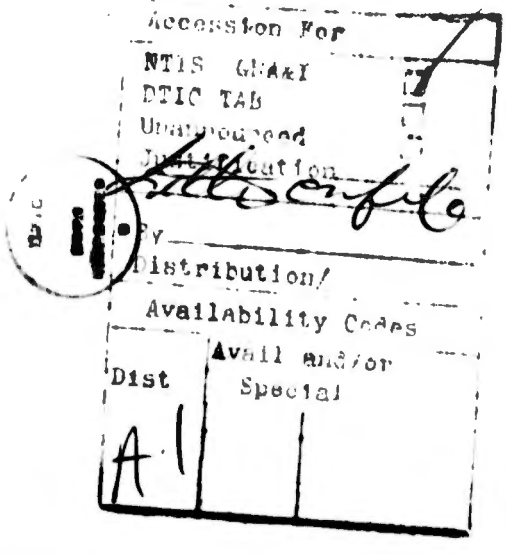

1.0 INTRODUCTION

1.1 Purpose - The purpose of this report is to presents the results of a contamination analysis on the Defense Support Program (DSP) satellite during launch and deployment by the Space Transportation System (STS). This report presents the predicted contaminant deposition on critical DSP surfaces during the period soon after launch when the DSP is in the Shuttle Orbiter bay with the doors closed, the bay-doors open and during initial deployment. Additionally, a six sided box was placed at the spacecraft position to obtain directional contaminant flux information for a general payload while in the bay and during deployment.

1.2 Scope - The analysis included contamination sources from the Shuttle Orbiter, IUS and cradle, the DSP sensor and the DSP support package.

During the period in bay-doors closed (one hour duration), the outgassing from all surfaces in the payload bay including the IUS and spacecraft were considered as sources. During the period in bay-doors open (2 hours duration), additional sources in the form of VCS engines and return flux of contaminants were considered. During deployment (~15 minutes), only Shuttle Orbiter fluxes on DSP critical surfaces were considered.

Critical surfaces (15 total) on the DSP that were evaluated are:

a) four second surface thermal mirror panels on the W71 sensor, (two of the mirror panels encompass the photoelectric cell radiators);
b) star sensors, (2);
c) cylindrical solar panels, (4 quadrants);
d) Radec ABL Systems, and
e) four surfaces perpendicular to the long axis of the spacecraft near the ABL area.

Off nominal periods of 4.5 hours in bay-doors closed and 24 hours in bay-doors open were also assessed. The variation in return flux during the in bay-doors open period for small attitude changes was evaluated.

1.3 Approach - The approach taken for this study was to utilize an existing DSP configuration used on a previous similar study and the Shuttle Orbiter configuration and data banks as

contained in the Shuttle/Payload Contamination Evaluation (SPACE) Program. In addition, sets of vacuum system equations were utilized in performing the in bay-doors closed analysis.

The comparison between the present study and a previous study performed 2 years ago is shown in Figure 1. The source characteristics and analysis techniques have been improved for the present study. Wherever possible, direct test results have been incorporated.

1.4 Summary - Potential deposition levels on specific sensor surfaces were evaluated and the results indicate:

- maximum baseline deposition on any critical surfaces is approximately 10Å;
- DSP surfaces were warm enough to prevent net deposits of:
  - early desorption products,
  - cabin leakage,
  - flash evaporator exhaust and
  - major portions of engine exhaust;
- VCS engine deposits were less than 1Å;
- major deposition occurred during the in bay-doors closed period and the in bay-doors open and
- deployment is a relatively clean period--deposits less than 1Å.

2.0 MODELED CONFIGURATIONS

2.1 Modeling Approach - The spacecraft and Shuttle Orbiter were modeled on a CDC 6000 series computer in terms of basic geometric shapes. The relations between the DSP critical surfaces and all other DSP, IUS and Shuttle surfaces were calculated at all relative positions modeled. The basic Shuttle Orbiter configuration used is as presented in detail in the "Shuttle/Payload Contamination Evaluation Program" Users Manual, MCR-77-106, April 1977. The only changes made for this analysis were in the payload bay liner nodal structure which was increased from 8 to 16 nodes and the payload filters were included in the payload bay liner. These changes were required for improved resolution

PRESENT	PAST *
• ONE HOUR IN BAY-DOORS CLOSED EXPOSURE	• 11 MINUTES IN BAY-DOORS CLOSED EXPOSURE
• 2 HOURS IN BAY-DOORS OPEN EXPOSURE	• ONE HOUR AND 45 MINUTES IN BAY-DOORS OPEN EXPOSURE
• 917 SECONDS DEPLOYMENT EXPOSURE	• 460 SECONDS DEPLOYMENT EXPOSURE
• ALTITUDE 160 NAUTICAL MILES	• ALTITUDE 160 NAUTICAL MILES
• VELOCITY VECTOR PARALLEL TO X AXIS	• VELOCITY VECTOR PARALLEL TO X AXIS
• IMPROVED SPECIFIC SOURCE CHARACTERISTICS	• GENERALLY APPLIED SOURCE CHARACTERISTICS
• TESTING PERFORMED TO SUPPORT ANALYSIS	• NO TESTING PERFORMED
• IMPROVED ANALYSIS TECHNIQUES - IN BAY AND RETURN FLUX	• NO SPACECRAFT (PAYLOAD) CONTRIBUTIONS
• IMPROVED TEMPERATURE RELATIONS	
• DSP CONSIDERED AS A SOURCE	
• IMPROVED IUS GEOMETRY	

* Contamination Subcontract Study
DOD Space Transportation Study (STS)
Payload Interface Support Study
January 1976, MCR 76-12, MDAC
0067671H, Martin Marietta Aerospace

Figure 1 Comparison Between Present/Past Studies

in determining viewfactors and for shadowing considerations.

2.2 DSP Configuration - The DSP satellite was represented by 33 surfaces, 15 of which were considered as critical surfaces. Other surfaces not considered sensitive to contamination were included to properly account for the transport of contaminants. Figure 2 shows the modeled DSP configuration with the critical surfaces identified by node numbers for reference to the following contamination predictions.

2.3 IUS Configuration - The IUS configuration was represented by a total of 26 surfaces. This number was sufficient for outgassing source characterization and shadowing considerations. Figure 3 shows a computer drawn graphic displays of the IUS DOD/NASA two stage configuration used in this study. Also shown are the 2 dimensional cradle components and the IUS integrated with the DSP spacecraft.

2.4 Integrated Configuration - The DSP position in the Shuttle Orbiter bay is shown in Figure 4. This relative position was used for the in bay-doors closed and the in bay-doors open analysis.

2.5 Deployment Positions - The DSP/IUS deployment sequence was supplied by NASA-JSC and is shown schematically in Figure 5. Viewfactors between the DSP critical surfaces and the Shuttle Orbiter were calculated for each of these positions for contamination predictions.

3.0 MISSION PROFILE

3.1 Nominal Mission - The nominal mission profile defined for this study consisted of three major flight segments which were:

a)	IN BAY - DOORS CLOSED	ONE HOUR (3600s)
b)	IN BAY - DOORS OPEN	TWO HOURS (7200s)
c)	DEPLOYMENT	917 SECONDS TOTAL

During all of these intervals, the Shuttle Orbiter was held in a fixed attitude (bay looking at the earth) in a fixed ZLV mode at a zero degree beta angle. At this attitude, the velocity vector is parallel to the Shuttle Orbiter X axis. The temperatures for this attitude were supplied by Rockwell International

33 SURFACES

15 CRITICAL

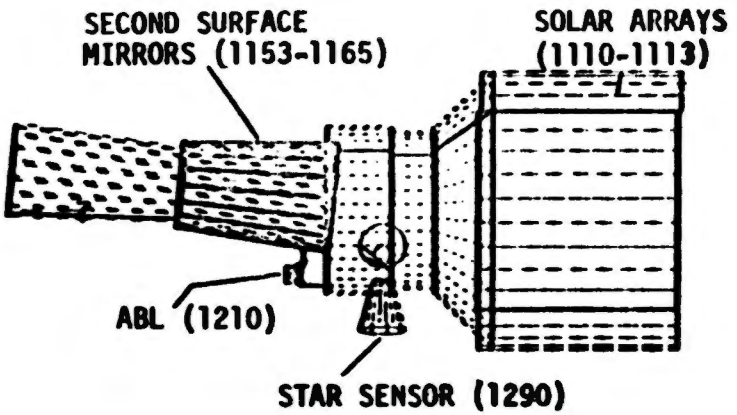

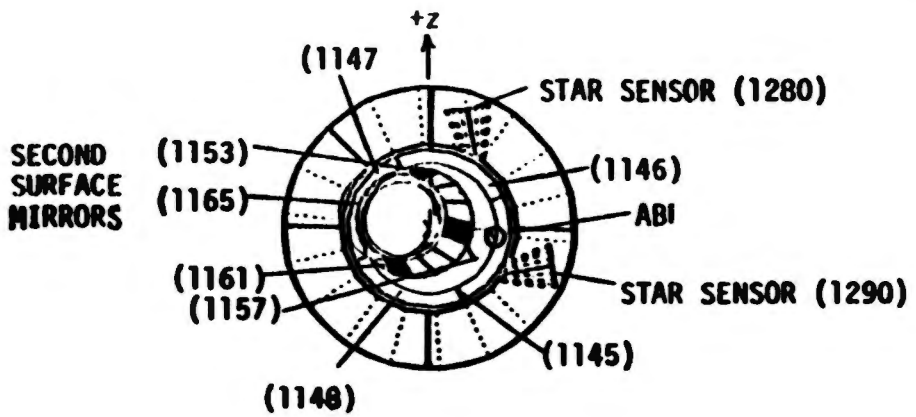

Figure 2 DSP Surfaces

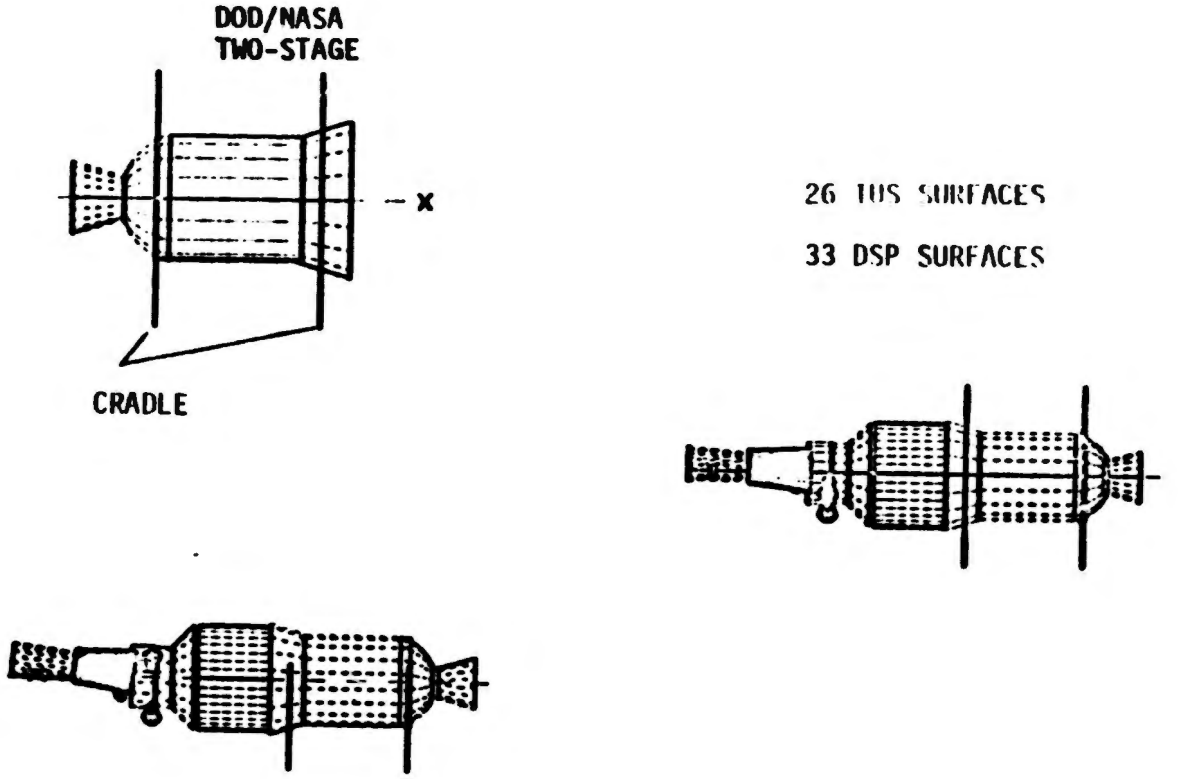

Figure 3 IUS Configuration

TOTAL 312 NODES

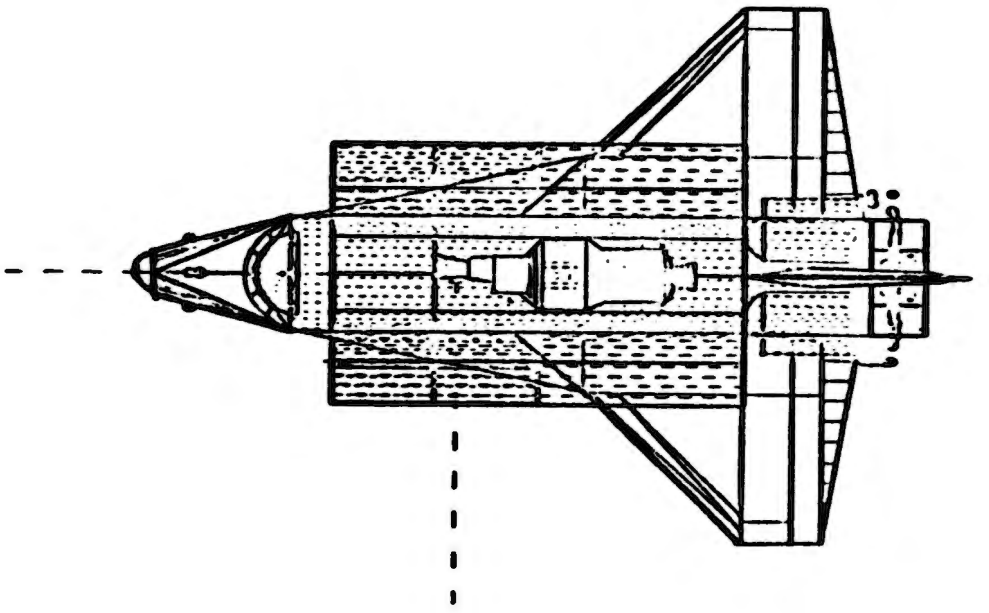

Figure 4 Integrated Configuration

STATION ONE	STATION TWO	STATION THREE	STATION FOUR	STATION FIVE
69.5 SECONDS	193 SECONDS	387.5 SECONDS	193 SECONDS	74 SECONDS
12 FEET ALONG z	90 DEGREES ABOUT z	180 DEGREES ABOUT -y	90 DEGREES ABOUT -z	13 FEET ALONG z

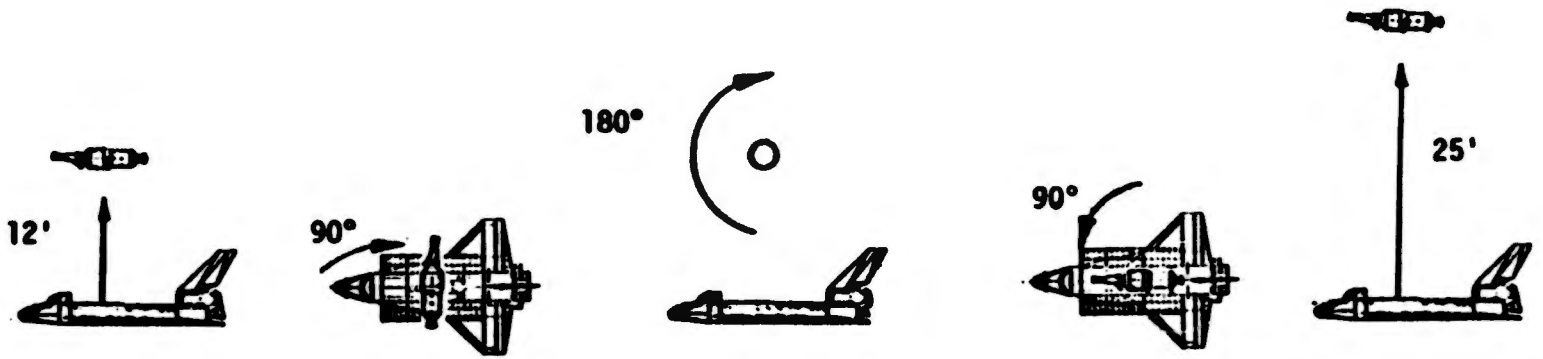

Figure 5 Deployment Positions

for both the doors open and closed case. The mission altitude was defined as 160 nm (296 km) which is important for return flux calculations.

3.2 Off Nominal Mission - The off nominal mission contingency modes were defined as:

a) IN BAY - DOORS CLOSED 4.5 HOURS (1.56×10^4 s)

b) IN BAY - DOORS OPEN 24 HOURS (8.64×10^4 s)

The attitude and altitude for the off nominal cases were the same as the nominal case.

An additional off nominal parameter considered was to vary the angle the velocity vector makes with the Z axis. Nominally, it is at 90 degrees with respect to the Z axis. The off nominal situations analyzed were at 60 degrees and 120 degrees, still in the X-Z plane. This provides an indication of the potential variation in return flux as a function of angle of attack for the Shuttle Orbiter and is presented later in the following results section.

4.0 RESULTS

4.1 In Bay-Doors Closed - The following analysis was used to establish the in bay-doors closed contamination predictions for the DSP.

4.1.1 Payload Bay Pressures - To analyze the payload bay-doors closed case, the pressure must be calculated to determine if free molecular flow from surface to surface exists or if a random, diffuse gas mixing situation exists. The payload bay equilibrium pressure, soon after launch, is dictated by the pressurized cabin leakage which consists of H_2O, N_2, O_2 and CO_2. The specified leak rate is 7 lbs·day^{-1} or 21.7 Torr·l·s^{-1}, half of which is assumed to leak into the payload bay volume and the rest into the volume between the payload bay liner and outer fuselage region. The resulting pressure can be calculated from equations supplied by JSC which incorporate the pumping speed of the overboard conductances. This is expressed as

$$P = 0.0343\ Q_1 + 0.038\ Q_2$$

where

Q_1 = bay input (upper mid-fuselage), $Torr \cdot m^3 \cdot s^{-1}$ and

Q_2 = input between liner and Orbiter bulkhead (lower mid-fuselage).

For the bay calculation, Q_1 and $Q_2 = 11 \times 10^{-3}$ $Torr \cdot m^3 \cdot s^{-1}$ and the pressure is $P = 8 \times 10^{-4}$ Torr.

At these pressures, the mean free path of a molecule is on the order of centimeters as compared to several or tens of meters separating the surfaces in the payload bay. Because of this, a random gas mixing is assumed so that all surfaces in the bay can be impinged upon from all sources. The additional effect of gas release by surfaces and total mass loss by non-metallics would be to increase the overall pressure by a small amount. This gas load amounts to less than 0.3 $Torr \cdot l \cdot s^{-1}$, which is a small quantity compared to the cabin leakage. This was obtained by averaging the TML rates in Table I.

To calculate the partial pressure of the volatile condensible material (VCM), an additional pumping speed must be calculated. This term accounts for the removal of the VCM by surfaces that are cool relative to the VCM source material. To calculate the pumping speed, the impingement rate on a surface must be determined.

The impingement rate on a surface area can be expressed as

$$\frac{dN}{dt} = 1/4 \, v_a \, nA$$

where

N = number of molecules,

n = number density of gas,

v_a = mean molecular speed and

A = pumping area of the surface.

By definition, the mass flux

$$Q = \frac{PdV}{dt} = kt \frac{dN}{dt}.$$

Substituting the previous expression for dN/dt and P = nkt into the above relationship, this yields

$$Q = 1/4\ v_a\ AP.$$

From this expression, the term $1/4\ v_a\ A$ is the pumping speed of the walls impinged upon for unit condensation coefficient. This situation is somewhat analogous to a cryo-wall condensing out gases in a vacuum system and represents a near maximum case when considering the VCM molecules are mixed with a larger amount of noncondensible gases. The reasoning here is that the VCM species will condense out on surfaces near 25°C.

By substituting

$$v_a = \left(\frac{8\ R_o\ T}{\pi M}\right)^{1/2}$$ in the above relationship, the pumping speed expression

$$S = \frac{v_a\ A}{4} \text{ becomes } S = \left(\frac{A R_o T}{2\ \pi\ M}\right)^{1/2} = 3.64\ A \left(\frac{T}{M}\right)^{1/2}\ l \cdot s^{-1}$$

where

A = area in square centimeters,

T = temperature in degrees Kelvin and

M = molecular weight of the molecule in grams per mole.

For air at 300°K, the pumping speed is S = 11.7A for a molecular weight of 29 $g \cdot mole^{-1}$. For the payload bay situation, the area of the liner and payload is $2.02 \times 10^6 cm^2$ which results in an effective pumping speed of

$$S = 2.4 \times 10^4\ m^3 \cdot s^{-1}$$

for a molecular weight of 29 $g \cdot mole^{-1}$ and $1.27 \times 10^4\ m^3 \cdot s^{-1}$ for a molecular weight of 100 $g \cdot mole^{-1}$. Because the pumping speed is much larger than the liner filter pumping speed, the pressure equation becomes

$$P = \frac{Q}{S} = \frac{Q}{1.27 \times 10^4}$$

where

Q = VCM mass input rate to the bay volume.

4.1.2 Payload Bay Sources - The remaining parameter to determine is the VCM input to the payload bay volume. Table I shows a compilation of the nonmetallics on the IUS/DSP and Shuttle Orbiter utilized for this study. Where materials data was unavailable, the general approach was to use the TML/VCM measurements made on these materials to estimate mass loss rates. The standard TML/VCM test time of 24 hours was used to obtain an average rate for the TML source temperature of 125°C and the VCM rate for a collector plate at 25°C. This data is currently the only extensive data for nonmetallics that is performed under similar test conditions. This approach results in a rate that is too low for initial vacuum exposure (first 1 to 3 hours) and too high for rates at the end of 24 hours. Wherever possible, the TML/VCM data was replaced or augmented by actual test data on the nonmetallics in question so that the results would be as accurate as possible.

An additional requirement was to reduce the mass loss rate for temperatures of the nonmetallics other than the standard TML test temperature of 125°C. Testing was performed to determine the change in mass loss rates as a function of source temperature for major sources. The testing was performed on Shuttle Orbiter sources (bulkhead TG-15000, silver Teflon adhesive and a silicone used on electrical connectors) and on major payload sources (epoxy laminate and Kynar wiring insulation). The testing for the materials had as its objective to determine mass loss rates at various temperatures anticipated during the mission, the time dependency of the outgassing rates and the effect on VCM of thermal vacuum testing of payload components prior to installation into the Shuttle Orbiter bay. This testing was performed at NASA-JSC in response to the need to determine parameters that would have a major impact on payload contamination predictions.

4.1.2.1 Orbiter Sources - The following data presents the results of testing performed by JSC in establishing the rates used for the Shuttle Orbiter sources. Initially, the data is presented for a first flight Orbiter and secondly, the reduction in rates due to previous vacuum exposure is also presented. The previous vacuum exposed Orbiter is considered as the baseline case. The Orbiter nonmetallics discussed previously were

TABLE I NONMETALLIC MASS LOSS RATES BASED ON VCM/TML AND TOTAL MASS AVAILABLE

NONMETALLIC MATERIAL	% TML	% CVCM	WEIGHT		AVERAGE CVCM MASS LOSS RATE @ 125°C/24 HRS. M=10		TML/VCM DATA SOURCE
			lbs	g	$g \cdot s^{-1}$	$Torr \cdot l \cdot s^{-1}$	
IUS - EXTERNAL							CORRESPONDENCE FROM H. MARTINEDES ESTEC, TO A. GALZERANO NASFC, DATED 12/27/77, REF. LS/HM/887
. CHEMGLAZE IIA-276	1.73	.003	4.5	2.04×10^{3}	7.10×10^{-7}	1.21×10^{-4}	
DSP (TRW) - EXTERNAL							OBTAINED FROM "COMPILATION OF VCM DATA OF NON-METALLIC MATERIALS" JSC 08962 REV O DECEMBER 1977
. DC93-072	1.67	0.60	.238	1.1×10^{2}	7.64×10^{-6}	.0013	
. EPOXY/DTA/HECRO BALLOON	2.42	.085	2.11	9.58×10^{2}	9.42×10^{-6}	1.6×10^{-3}	
. DC R-63-489	1.1	.67	5.88	2.67×10^{3}	1.45×10^{-4}	2.5×10^{-2}	
. DC3145	1.74	.75	7.41	3.36×10^{3}	2.92×10^{-4}	5.0×10^{-2}	
. 2R-852 or 2R-447	.75 1.15	.02 .11	.374 .374	1.69×10^{3} 1.69×10^{3}	3.91×10^{-6} 2.15×10^{-5}	6.7×10^{-4} 3.7×10^{-3}	
. FINCH 463-1-8 FLAT BLACK	UNKNOWN	UNKNOWN	.325	1.48×10^{2}	—	—	
. FINCH 643-1-1	UNKNOWN	UNKNOWN	.106	48	—	—	
INTERNAL (VENTED)							
. FINCH 463-1-8	UNKNOWN	UNKNOWN	1.35	6.13×10^{2}	—	—	
. DC3145	1.74	.75	2.09	9.49×10^{2}	8.24×10^{-5}	1.4×10^{-2}	
. 3M SCOTCH CAST 9	3.6	.04	1.12	5.1×10^{2}	2.36×10^{-6}	4×10^{-4}	
INTERNAL (PARTIALLY VENTED)							
. REV8111	1.19	.35	.14	63.6	2.58×10^{-6}	4.4×10^{-4}	
. 3M SCOTCHCAST 9	3.6	.04	6.1	2.77×10^{3}	1.28×10^{-5}	2.2×10^{-3}	
DSP (TRW) - MISCELLANEOUS MATERIALS							SUPPLIED BY TRW TO NASA JSC
. KYNAR INSULATION ON WIRING	.21	.02	31	1.41×10^{4}	3.26×10^{-5}	5.55×10^{-3}	
. FM123-5 (ON SOLAR PADDLE HONEYCOMB SANDWICH)	.78	.07	12	5.43×10^{3}	4.42×10^{-5}	7.52×10^{-3}	
. EPOXY LAMINATING RESIN	.4	.02	18.7	8.5×10^{3}	1.97×10^{-5}	3.35×10^{-3}	
ORBITER BAY							SUPPLIED BY NASA JSC
* . TG-15000 BULKHEAD INSULATION	.47	.049	87	3.95×10^{4}	2.20×10^{-4}	3.81×10^{-2}	
. ADHESIVE FOR Ag-FEP RADIATORS	.33	.21	40	1.81×10^{4}	4.41×10^{-4}	7.51×10^{-2}	
* . MLI BLANKETS	UNKNOWN	UNKNOWN	—	—	—	—	
* . SUPER KOROPON	5.47	0.1	—	—	—	—	
. BAY LINER	UNKNOWN	UNKNOWN	—	—	—	—	
DSP (AESC)	UNKNOWN	UNKNOWN	(VCM ONLY) 4.4×10^{-4}	(VCM ONLY) 0.2	2.30×10^{-6}	3.90×10^{-4}	SUPPLIED BY AESC

*THESE MATERIALS EXIST BETWEEN THE LINER AND THE LOWER MID FUSELAGE AND PRESENT NO PROBLEM BECAUSE OF LIMITED CONDUCTANCE TO THE BAY VOLUME AND CONDENSING SURFACES IN THE MID FUSELAGE REGION

tested for time and temperature dependence of VCM mass loss rates. Figure 6 shows the VCM curves for an RTV used on electrical connectors. The interesting feature here is the reduction in VCM by only a factor of two when the source temperature is reduced from 125°C to 40°C. It also shows that the majority of VCM is released during the first 2 to 3 hour period of vacuum exposure.

Figure 7 shows the VCM mass loss data obtained for the silver Teflon radiator surfaces on the payload bay doors. The dashed lines correspond to the silver Teflon bonded to an aluminum substrate and the solid lines correspond to no substrate with the adhesive exposed. The results show that the Al bonded sample mass loss was only 80% of the unbonded sample where the adhesive was totally exposed. Also, the reduction by approximately two is evident between source temperatures at 125°C and 48°C.

The adhesive for the door radiators is 0.003 inches thick (0.008 cm). For a density of 1.2 $g \cdot cm^{-3}$ and a total radiator area of 1.89×10^{6} cm^{2}, the total adhesive mass is 1.81×10^{4} g. From Table I, the VCM is 0.21% so that the mass available for VCM is 38g. Averaged over 24 hours and reduced by a factor of two, to account for temperature; the VCM mass loss rate is 2.2×10^{-4} $g \cdot s^{-1}$. Testing has shown (Figure 7) that the bonded configuration is 80% of the bare adhesive, so the rate reduces to 1.76×10^{-4} $g \cdot s^{-1}$ or equivalently, 3.74×10^{-2} $Torr \cdot l \cdot s^{-1}$ for a mass of 100 $g \cdot mole^{-1}$. The VCM molecular weight of 100 $g \cdot mole^{-1}$ was used in this analysis as an assumed average value. Testing shows masses that range from the 70 $g \cdot mole^{-1}$ to 170 $g \cdot mole^{-1}$ predominate at temperatures near 40°C. This rate was used in the analysis for in bay-doors closed for a first flight Orbiter.

Mass loss data for the bulkhead TG-15000 material is shown in Figure 8. This mass loss rate data is for the insulation material with no covering around it and, therefore, represents a maximum rate situation. These curves show that the majority of the mass is gone after 10 to 20 hours of exposure and also shows a reduction of approximately a factor of two for the total mass loss rate curves between 125°C and room temperatures. VCM/TML tests show that 10% of the total mass loss is VCM. Because actual rate data from testing is available for this material, it was used instead of average rates from Table I. The mass loss rate at the 10 hour point was chosen to be indicative

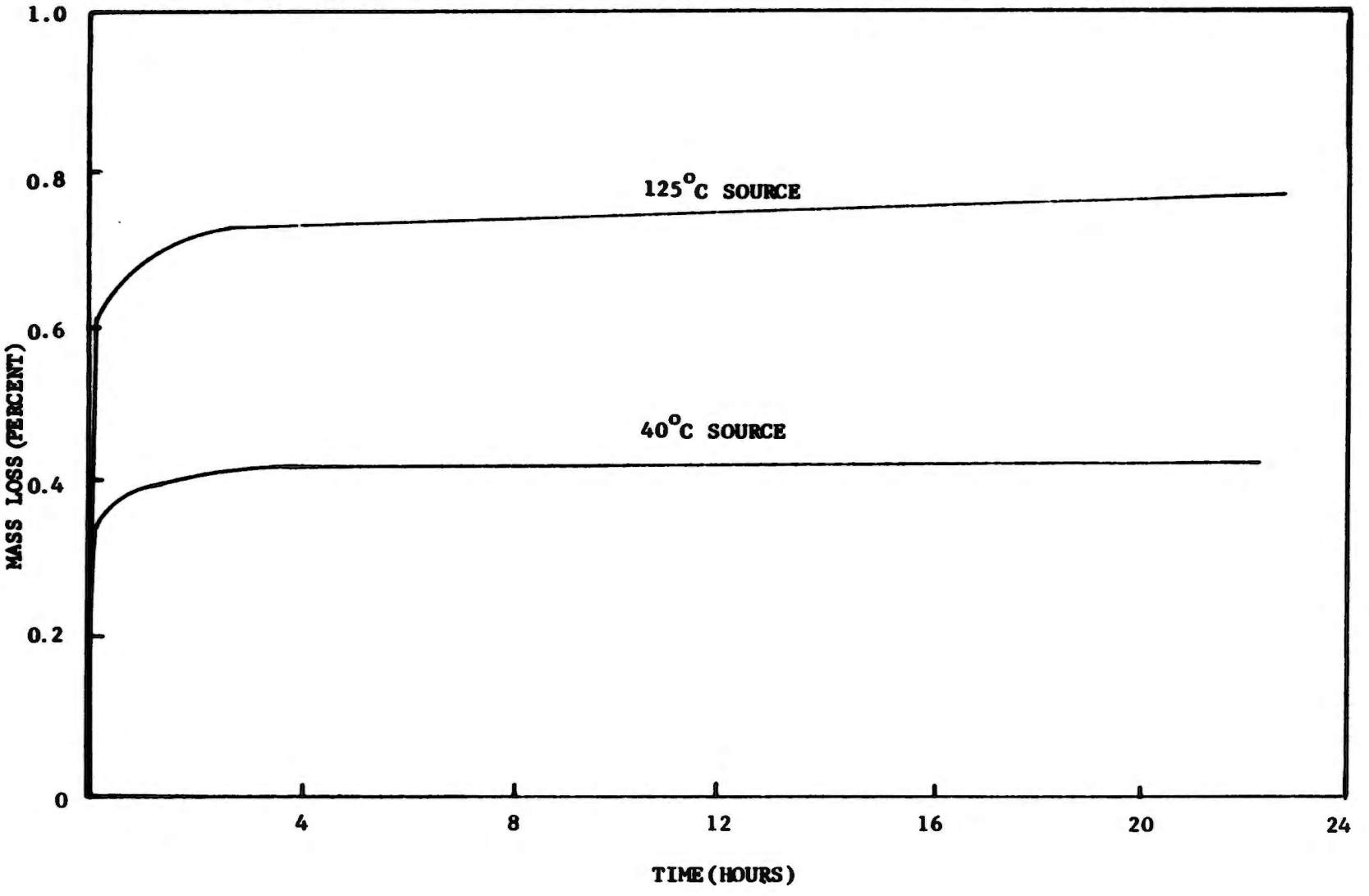

Figure 6 VCM Mass Loss for RTV Silicone from Cannon Electrical Connector, ME 414-0611-002

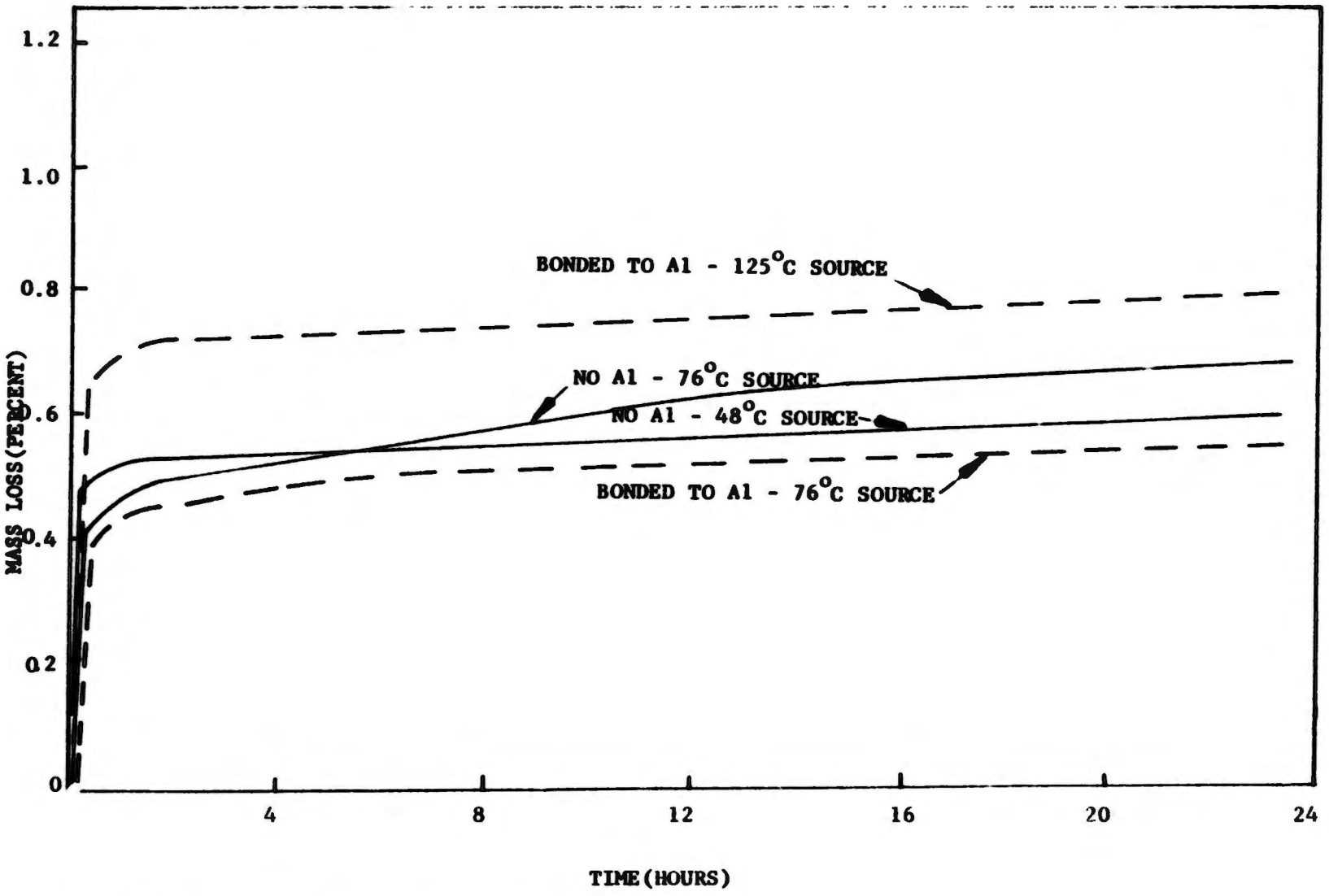

Figure 7 VCM Mass Loss For Silver Teflon Material With Adhesive

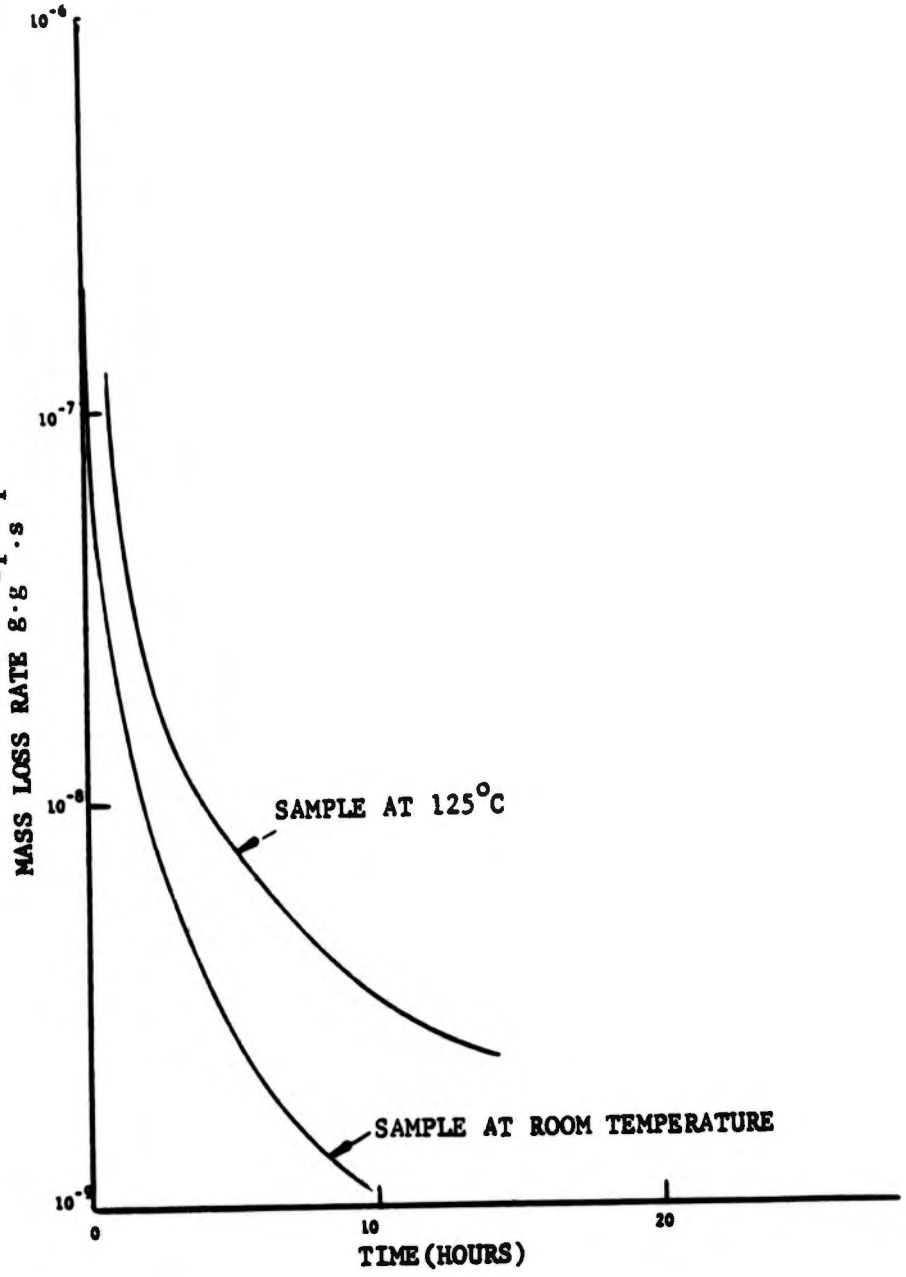

Figure 8 TG-15000 Mass Loss Rate Data

of a first flight Orbiter. At the 10 hour point, the TML rate is 6.8×10^{-7} Torr·l·s^{-1} at 125°C with a corresponding VCM of 6.81×10^{-8} Torr·l·s^{-1} per gram of material. For the total 87 pounds of insulation material (3.95×10^{4} g), this equates to a VCM mass loss rate of 2.69×10^{-3} Torr·l·s^{-1} at 125°C. Since the bulkhead will be near 40°C during operation, this rate should be reduced by a factor of two, as shown by testing, so that the VCM mass input rate to the payload bay volume is 1.34×10^{-3} Torr·l·s^{-1}. This rate was used for the in bay-doors closed analysis for a first flight Orbiter.

The payload bay liner of the Orbiter will not have a VCM content of any sigrificance. The material is an 8 oz. per sq. yd. Teflon coated beta cloth. Testing has shown that the mass loss rate, after only 1 - 5 hours vacuum exposure, is below 10^{-11} g·cm^{-2}·s^{-1} and is comprised mainly of the desorption of simple adsorbed atmospheric gases.

The super koropon, used as a coating on internal structures of the Shuttle Orbiter under the palyload bay liner, has a TML of 5.47% and a VCM of 0.1%. Subsequent testing at JSC has shown that the TML may be as high as 10% and does fluctuate from sample to sample. Any VCM mass loss from this source must enter the bay volume through the filtered openings between the liner and the mid-fuselage region. The amount entering through these filtered vents is small compared to sources within the bay volume. Additionally, the majority of VCM will condense onto the outside of the payload bay liner and other internal structure.

The TG-15000 and MLI blankets that exist between the payload bay liner and outer fuselage do not contribute significantly into the bay volume for the same reasons given for super koropon above. Because it is very unlikely that a sensitive payload will ever fly on a virgin Orbiter, it remains to determine the effect of vacuum exposure on Orbiter sources from flights previously completed. A previously vacuum exposed Orbiter was considered as the baseline situation for this study. It is estimated that at least one or two equivalent 7 day on-orbit missions will have been flown before sensitive payloads are placed in the Orbiter. By reviewing the long term thermal vacuum exposure of DSP components, (see Figure 9), it appears the reduction would be to a level on the order of 1×10^{-10} g·g (parent material)$^{-1}$·s^{-1}. That is to say that the rate for the Kynar did not exceed the minumum detectable limit of 1×10^{-10} g·g^{-1}.s^{-1} for a 48 hour period. This assumption appears valid in light

of the data presented in Figures 6, 7, and 8 for periods of 24 hours. These curves show a significant reduction in mass loss after a relatively short 24 hour period. Based on this, the mass input of the Orbiter sources is ($1x10^{-10}$ g·g (material)$^{-1}$·s^{-1}) ($5.8x10^{4}$ g (material)) = $5.8x10^{-6}$ g·s^{-1} or equivalently $9.8x10^{-4}$ Torr·l·s^{-1} for a molecular weight of 100 g·mole^{-1}. This rate was used for the in bay-doors closed baseline analysis of a previous flight exposed Orbiter source input.

4.1.2.2 IUS Sources - The major IUS source identified is the Chemglaze IIA-276 external white thermal control paint. Testing has shown that the TML of this paint at 40°C for 160 hours is 1.73% and the VCM collected at 25°C is reported to be less than 0.003%. The area of the exterior of the IUS is $2.66x10^{5}$ cm^{2}. For an anticipated application thickness of 0.008 cm (.003 in) and a unit density, the total mass is $2.13x10^{3}$g. If the TML/VCM data is averaged over a 24 hour period, which shows the major mass loss, the mass loss rate at 40°C is $1.26x10^{-4}$ Torr·l·s^{-1} for the VCM. This rate was used in the in bay-doors closed analysis. The IUS engine casings are comprised of a Kevlar material in an epoxy matrix. Even though this source is near 400 lb, VCM testing shows a zero measurement of VCM.

4.1.2.3 DSP-AESC Sources - The sources from the sensor portion of the DSP were specified by AESC to be 1.73 g of VCM available before thermal vacuum testing. After thermal vacuum testing, the remaining VCM was specified by AESC to be less than 0.2 g. If this were averaged over a 24 hour period, the rate would be $2.3x10^{-6}$ g·s^{-1} or equivalently $3.93x10^{-4}$ Torr·l·s^{-1} at 125°C and scaling by a factor of two gives $1.97x10^{-4}$ Torr·l·s^{-1}. This rate was used for in bay-doors closed analysis.

4.1.2.4 DSP-TRW Sources - The support package portion of the DSP has a great deal of nonmetallic materials as shown in Table I. The total mass loss rate at 40°C for these sources was determined to be $3.17x10^{-4}$ g·s^{-1} or $5.4x10^{-2}$ Torr·l·s^{-1}. The TRW portion of the DSP undergoes vacuum checkout for a period of 6 days at ambient temperature. To determine what effect this has on VCM removal during thermal vacuum testing, several of the major components were tested at JSC. Figure 9 shows the results for the Kynar wiring insulation and the epoxy laminate resin. The data shows that the mass loss rate decreases significantly with time at room temperature in vacuum. The Kynar rate initially is $1.1x10^{-6}$ g·s^{-1} (Figure 9) and at 120 hours

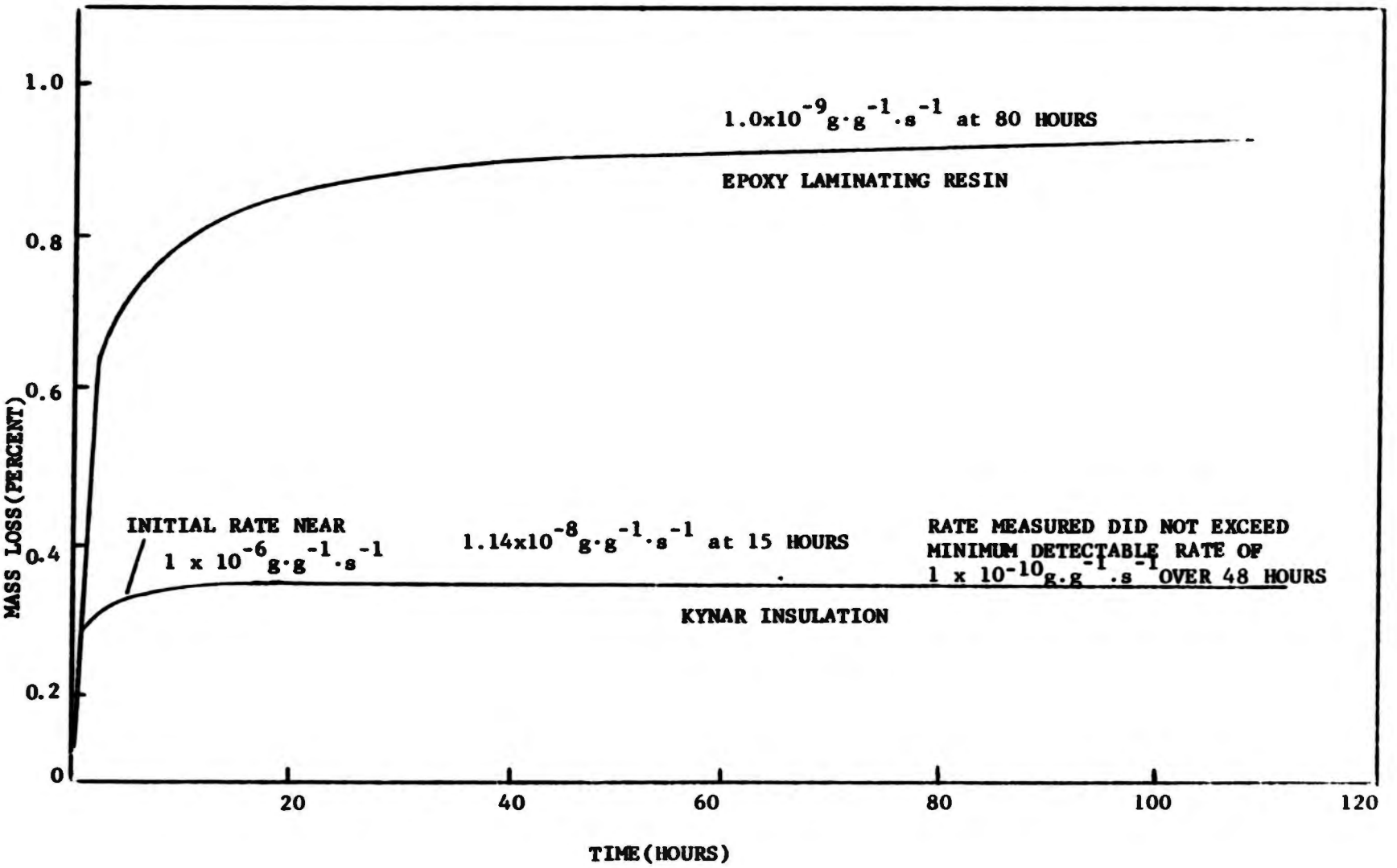

Figure 9 Mass Loss for Epoxy Laminate and Kynar Insulation(Room Temperature)

is undetectable but has been estimated to be $1x10^{-10}$ $g \cdot g^{-1} s^{-1}$, Figure 9. For a reported available mass of $1.41x10^{4}$ g of Kynar, the total mass loss rate at 25°C after 80 hours in vacuum would be $1.41x10^{-6}$ $g \cdot s^{-1}$. This term is different than that presented in Table I but was used since the test data on long term behavior is more desirable than an averaging technique based on VCM. After long exposure in vacuum, the fraction of the total mass loss that is VCM is larger than the ratio of VCM to TML would indicate. This results from the fact that the lighter gases come off much faster than the outgassing, large molecular weight components. It was assumed that one half of the mass loss after 80 hours was VCM. Therefore, the VCM mass input for Kynar is $7.3x10^{-7}$ $g \cdot s^{-1}$ or equivalently $1.24x10^{-4}$ $Torr \cdot l \cdot s^{-1}$.

The epoxy laminate curve in Figure 9 shows a mass loss rate of $1.0x10^{-9}$ $g \cdot g^{-1} \cdot s^{-1}$ at the end of 80 hours in vacuum at 25°C. This equates to a TML of $8.5x10^{-6}$ $g \cdot s^{-1}$. Once again, it was assumed half of this is VCM so the VCM rate is $4.3x10^{-6}$ $g \cdot s^{-1}$ or equivalently $7.24x10^{-4}$ $Torr \cdot l \cdot s^{-1}$ for the $8.5x10^{3}$ g of epoxy resin.

The rates calculated for the VCM of the two above materials were used for the in bay-doors closed analysis, The Kynar and epoxy laminate compromise 56% of the TRW nonmetallics. There was insufficient time to test all of the remaining TRW materials under thermal vacuum preflight test conditions. It is reasonable to assume that the rates for the remaining 39.6 lb ($1.8x10^{4}$ g) would be near $1x10^{-9}$ $g \cdot g^{-1} \cdot s^{-1}$, the same as for the epoxy laminate. This results in a VCM input (assuming once again that half the mass loss at 80 hours is VCM) of $9x10^{-6}$ $g \cdot s^{-1}$ or equivalently $1.53x10^{-3}$ $Torr \cdot l \cdot s^{-1}$.

Based on these assumptions and tests discussed previously, the total VCM input to the payload from the DSP-TRW nonmetallics is $2.38x10^{-3}$ $Torr \cdot l \cdot s^{-1}$.

4.1.3 Resulting Deposition - The deposition results for the in bay-doors closed case are presented in Table II along with the VCM mass inputs from the major sources. As shown, the effects of a previously vacuum exposed Orbiter is to significantly reduce the VCM input to the payload bay volume and the resulting deposition. It should be noted that if some of the payload bay surfaces were not capable of condensing part of the VCM, the deposition would be greater.

TABLE II VCM MASS INPUT AND DEPOSITION RESULTS - IN BAY-DOORS CLOSED

Source	VCM Input Rate $g \cdot s^{-1}$	VCM Input Rate $Torr \cdot l \cdot s^{-1}$	% Contribution Previously Flown Orbiter	% Contribution Initial Flight Orbiter	Remarks/Comments
IUS	7.38×10^{-7}	1.26×10^{-4}	3	<1	Thermal vacuum testing not accounted for - TML/VCM data questionable
DSP-AESC	1.16×10^{-6}	1.97×10^{-4}	5	<1	Thermal vacuum testing accounted for - VCM reduced to 12% of non-vacuum exposed materials
DSP-TRW	1.4×10^{-5}	2.38×10^{-3}	65	6	Thermal vacuum exposure of 6 days at room temperature accounted for from testing at JSC
Orbiter (Previously flown)	5.8×10^{-6}	9.84×10^{-4}	27	-	A first flight orbiter refers to average rates during a 24 hour period of a first flight - previously flown refers to approximately a seven day mission on-orbit exposure and uses the attenuation found in testing of DSP-TRW materials
(First Flight)	2.29×10^{-4}	3.89×10^{-12}	-	93	
TOTAL Previously flown		3.69×10^{-3}	100		$P = Q/S \quad \frac{Q}{1.27 \times 10^{4}}$
First Flight		4.16×10^{-2}			
Resulting Deposition Previously Flown	$4\text{Å} \cdot hr^{-1}$				$\dot{m} = 5.83 \times 10^{-2} P_{VCM} \left(\frac{M}{T}\right)^{\frac{1}{2}}$ $g \cdot cm^{-2} \cdot s^{-1}$
First Flight	$45\text{Å} \cdot hr^{-1}$				

The resulting deposition was calculated from the Langmuir-Knudsen relationship

$$\dot{m} = 5.83\times10^{-2}\ P_{VCM}\left(\frac{M}{T}\right)^{1/2},\ g\cdot cm^{-2}\cdot s^{-1}$$

where

P_{VCM} = partial pressure of VCM,

M = molecular weight and

T = temperature.

The value of P_{VCM} was determined from

$$P_{VCM} = \frac{Q}{S} = \frac{3.69\times10^{-3}\ Torr\cdot l\cdot s^{-1}}{1.27\times10^{7}\ l\cdot s^{-1}} = 2.9\times10^{-10}\ Torr.$$

The value of $\dot{m}$ where M = 100 and T = 298K, is $9.76\times10^{-12}\ g\cdot cm^{-2}\cdot s^{-1}$ for the baseline case. For a 3600 second exposure, the net deposition is 4Å for unit density. For a first flight Orbiter, the deposition would be 45Å. The 45Å was calculated assuming no previous vacuum exposure.

The other sources in the form of cabin leakage and volatile species from nonmetallics have an impingement rate on DSP surfaces near $1.5\times10^{-5}\ g\cdot cm^{-2}\cdot s^{-1}$. This was calculated from the above $\dot{m}$ expression and a total bay pressure of 8×10^{-4} Torr. However, these molecular species will not condense at DSP surface temperatures and therefore present no long term deposition potential.

4.2 <u>In Bay-Doors Open</u> - During this exposure time, one major transport of contaminants is the molecular flow conditions from one surface to another unhindered by collisions occurring between the surfaces. The other major transport mechanism is the return flux of contaminants to spacecraft surfaces through interactions with the ambient atmosphere.

4.2.1 <u>Direct Flux</u> - The deposition from direct flux of contaminants on critical DSP surfaces during the in bay-doors open is less than one angstrom for all surfaces. Table III shows the deposition levels for the critical surfaces during this period. The only surfaces that directly see the DSP surfaces are the payload bay liner and the bulkhead area.

TABLE III LOCATION/DEPOSITION, (Å), IN BAY DOORS OPEN AND DEPLOYMENT

Node Number	Description	In Bay Doorg Open (7200 s) Å			Station 1 (69.5 s)	Station 2 (193 s)	Station 3 (387.5 s)	Station 4 (193 s)	Station 5 (74 s)	Total
DSP	Surface Nomenclature	Direct Flux Å	Return Flux* Out-gassing	Return Flux* VCS	Direct Flux Å	Direct Flux Å	Direct Flux Å	Direct Flux Å	Direct Flux Å	Å
1110	Solar Arrays	.045	6	<1	____	.0053	.034	.012	.0085	6.1
1111	Solar Arrays	.032	4	<1	.0042	.016	.02	.012	.0023	4.1
1112	Solar Arrays	.031	0		.0041	.0093	.0057	____	____	0.05
1113	Solar Arrays	.032	4	<1	.0042	.0028	.00011	.012	.0023	4.1
1153	OSR	.00017	6	<1	____	.000031	.0042	.0022	.001	6.0
1157	OSR	.043	0	0	.00087	.0024	.0045	.0017	.00022	0.05
1161	OSR	.017	0	0	.0012	.0022	.0012	____	____	0.02
1165	OSR	.042	0	0	.00058	.00063	.000098	.0027	.00048	0.05
1280	Star Sensor	.18	0	0	.0011	.0030	.011	.006	.0011	0.2
1290	Star Sensor	.072	0	0	.0027	.0056	.0093	.0029	.00084	0.1
1210	ABL	.00036	0	0	.00027	____	____	.0009	.00017	0.0
1145	Ring	.02	6	<1	.00049	.00068	.0012	.001	.00023	6.0
1146	Ring	.013	6	<1	.00022	.00026	.0013	.0015	.00037	6.0
1147	Ring	.015	6	<1	.00033	.00024	.0004	.0011	.0003	6.0
1148	Ring	____	0	0	.00052	.00062	.00053	.00076	.0092	0.01

* For a first flight Orbiter the outgassing return flux will be a maximum of 21Å on surfaces 1110, 1153, 1145, 1146 and 1147 and 15Å on surfaces 1111 and 1113.

Even though the time interval was 7200 seconds, the rates from these sources was low enough that no significant deposition occurred. At temperatures of 12°C, the mass loss rates of these sources was on the order of 4×10^{-11} $g \cdot cm^{-2} \cdot s^{-1}$.

Secondary reflections from the IUS/DSP to the Orbiter liner and back to DSP critical surfaces was not in scope with this study. However, it was preliminarily assessed and appears to be less than the rate of the Orbiter materials themselves and is thus considered as no problem.

4.2.2 Outgassing Return Flux - Other surfaces that do not see the DSP surfaces directly during the in bay-doors open period are the radiators and TPS surfaces of the Shuttle Orbiter as well as the IUS surfaces. These surfaces can contribute indirectly by interacting with the ambient atmosphere and scattering back to the DSP surfaces. Table IV shows the input control parameters used in operating the SPACE computer program. Table V is a listing of the mission parameters used in defining the vehicle attitude and altitude for the return flux calculations. Table VI shows the mass loss rates of the Shuttle Orbiter surfaces after they have been corrected for temperature. This table corresponds to report #11 from the SPACE computer program and indicates the total mass loss rate from a surface, the per unit area rate and finally a summary of the total mass loss rate from the Orbiter and the average rate for the Orbiter surfaces. The return flux calculated for these source rates and the nominal attitude are shown in Table VII. The total return flux is shown to be 2.2×10^{11} $molecules \cdot cm^{-2} \cdot s^{-1}$ or a mass impingement rate of 3.61×10^{-11} $g \cdot cm^{-2} \cdot s^{-1}$. Of this, 63.8% is from the radiators which have a maximum surface mass loss rate of 8.9×10^{-11} $g \cdot cm^{-2} \cdot s^{-1}$ as shown in Table VI. Since direct data was available for the radiators and TG-15000, it was used as input to the SPACE program. In addition to the Orbiter sources, the return flux from the IUS/DSP is 2.53×10^{-12} $g \cdot cm^{-2} \cdot s^{-1}$. This was determined by calculating what percentage of the Orbiter number column densities the IUS/DSP comprised. The results showed the IUS/DSP was 7% of the Orbiter return flux.

Since the VCM rate for the radiators and IUS/DSP sources was used, the condensation coefficient on payload surfaces below 25°C is unity. For the remainder of the Orbiter surfaces (NOMEX, LRSI and HRSI), the return flux is 1.3×10^{-11} $g \cdot cm^{-2} \cdot s^{-1}$ with a condensation coefficient near 0.3 for the 50°C sources

TABLE IV INPUT CONTROL PARAMETERS FOR RETURN FLUX CALCULATIONS

REPORT NO. 1 **** PETURN FLUX ****** 12/06/77 23.56.55. PAGE 1

CONTENTS: LISTING OF INPUT CONTROL PARAMETERS

```
$CONTRL
DBUGA    = F,
DBUGB    = F,
DBUGC    = F,
DBUGD    = F,
DEPSIT   = T,
ED       = F,
ENG      = F,
EVAP     = F,
FIVP     = F,
LEAK     = F,
LOOP     = F,
MAXTMP   = T,
MCD      = F,
MFPATH   = F,
NEWCON   = F,
NEWTNL   = F,
NEWMFP   = F,
NEWMFS   = F,
NEWMLC   = F,
NEWTCD   = F,
MINTMP   = F,
```

TABLE IV INPUT CONTROL PARAMETERS FOR RETURN FLUX CALCULATIONS - concluded

```
ORBITR  = T.
OUT     = T.
REFLCT  = F.
REPORT  = T. F. T. F. F. F. F. T. F. F. T. F. F. F. F. F. F. F. F. F. F. F. F.  F. F. F. F. F. F. F. T. T. F. F. F. F. F. F. F. F
          T. F. F. T. T. F. F. T.
RFAS    = T.
RFSS    = T.
SMTP    = F.
TSTART  = 0.0. .3E+01. 0.0.
TSTOP   = .2E+01. 0.0. 0.0.
ATCODE  = 0.0.
GO      = T.
$END
```

TABLE V MISSION DATA INPUT FOR RETURN FLUX CALCULATIONS

```
REPORT NO.  8  **** RETURN FLUX ******

CONTENTS:  LIST OF MISSION DATA THAT WILL BE USED

$MPDB

BETA    = 0.0,

PITCH   = 0.0,

YAW     = 0.0,

ROLL    = 0.0,

ALT     = .3E+03,

SUNL    = F,

SUNM    = T,

SUNH    = F,

VX      = .765E+04,

VY      = 0.0,

VZ      = 0.0,

NLOS    = 1,

XLOS    = .1107E+04, .1107E+04, .1107E+04, .1107E+04, .1107E+04, .1107E+04,     .1107E+04, .1107E+04, .1107E+04, .1107E+04,
          .1107E+04, .1107E+04, .1107E+04, .1107E+04, .1107E+04, .1107E+04,     .1107E+04, .1107E+04, .1107E+04, .1107E+04,
          .1107E+04, .1107E+04, .1107E+04, .1107E+04, .1107E+04,

YLOS    = 0.0, 0.0, 0.0, 0.0, 0.0, 0.0, 0.0, 0.0, 0.0, 0.0, 0.0, 0.0, 0.0, 0.0, 0.0, 0.0, 0.0, 0.0, 0.0, 0.0, 0.0,
          0.0, 0.0, 0.0, 0.0,

ZLOS    = .507E+03, .507E+03, .507E+03, .507E+03, .507E+03, .507E+03, .507E+03, .507E+03, .507E+03, .507E+03, .507E+03,
          .507E+03, .507E+03, .507E+03, .507E+03, .507E+03, .507E+03, .507E+03, .507E+03, .507E+03, .507E+03, .507E+03,
          .507E+03, .507E+03, .507E+03,

THETAL  = 0.0, .3E+02, .6E+02, .3E+02, .6E+02, .3E+02, .6E+02, .3E+02, .6E+02,   .3E+02, .6E+02, .3E+02, .6E+02, .3E+02,
          .6E+02, .3E+02, .6E+02, .825E+02, .825E+02, .825E+02, .825E+02,       .825E+02, .825E+02, .825E+02, .825E+02,
```

TABLE V MISSION DATA INPUT FOR RETURN FLUX CALCULATIONS - continued

```
PHIL* = 0.0, 0.0, 0.0, .45E+02, .45E+02, .9E+02, .9E+02, .135E+03, .135E+03, .19E+03, .18E+03, .225E+03, .225E+03,
        .27E+03, .27E+03, .315E+03, .315E+03, 0.0, .45E+02, .9E+02, .135E+03, .18E+03, .225E+03, .27E+03, .315E+03,

DSMCD = .25E+01, .5E+01, .5E+01, .5E+01, .5E+01, .5E+01, .5E+01, .5E+01, .5E+01, .5E+01, .15E+02, .25E+02, .375E+02,
        .5E+02, .124E+03, 0.0, 0.0, 0.0, 0.0, 0.0, 0.0, 0.0, 0.0, 0.0, 0.0,

RMAXL = .3E+03,

RFSURF = 1110, 1111, 0, 0, 0, 0, 0, 0, 0, 0,

COSXX = .1E+01, .1E+01, .1E+01, .1E+01, .1E+01, .1E+01, .1E+01, .1E+01, .1E+01, .1E+01,

COSXY = 0.0, 0.0, 0.0, 0.0, 0.0, 0.0, 0.0, 0.0, 0.0, 0.0,

COSXZ = 0.0, 0.0, 0.0, 0.0, 0.0, 0.0, 0.0, 0.0, 0.0, 0.0,

COSYX = 0.0, 0.0, 0.0, 0.0, 0.0, 0.0, 0.0, 0.0, 0.0, 0.0,

COSYY = .1E+01, .1E+01, .1E+01, .1E+01, .1E+01, .1E+01, .1E+01, .1E+01, .1E+01, .1E+01,

COSYZ = 0.0, 0.0, 0.0, 0.0, 0.0, 0.0, 0.0, 0.0, 0.0, 0.0,

COSZX = 0.0, 0.0, 0.0, 0.0, 0.0, 0.0, 0.0, 0.0, 0.0, 0.0,

COSZY = 0.0, 0.0, 0.0, 0.0, 0.0, 0.0, 0.0, 0.0, 0.0, 0.0,

COSZZ = .1E+01, .1E+01, .1E+01, .1E+01, .1E+01, .1E+01, .1E+01, .1E+01, .1E+01, .1E+01,

THETA1 = 0.0, 0.0, 0.0, 0.0, 0.0, 0.0, 0.0, 0.0, 0.0, 0.0,

THETA2 = .9E+02, .9E+02, 0.0, 0.0, 0.0, 0.0, 0.0, 0.0, 0.0, 0.0,

PHI1 = 0.0, 0.0, 0.0, 0.0, 0.0, 0.0, 0.0, 0.0, 0.0, 0.0,

PHI2 = .36E+03, .36E+03, .36E+03, .36E+03, .36E+03, .36E+03, .36E+03, .36E+03, .36E+03, .36E+03,

OMEGA = .5E+00, .5E+00, 0.0, 0.0, 0.0, 0.0, 0.0, 0.0, 0.0, 0.0,

DSRTNF = .25E+01, .5E+01, .5E+01, .5E+01, .5E+01, .5E+01, .5E+01, .5E+01, .5E+01, .5E+01, .15E+02, .25E+02, .375E+02,
         .5E+02, .124E+03, 0.0, 0.0, 0.0, 0.0, 0.0, 0.0, 0.0, 0.0, 0.0, 0.0,
```

TABLE V MISSION DATA INPUT FOR RETURN FLUX CALCULATIONS - concluded

```
DTHETA = .45E+02, .45E+02, 0.0, 0.0, 0.0, 0.0, 0.0, 0.0, 0.0, 0.0,
DPHI   = .1024E+02, .1024E+02, .1024E+02, .1024E+02, .1024E+02, .1024E+02,
         .1024E+02, .1024E+02, .1024E+02, .1024E+02,
RMAXRF = .3E+03,
RFSTK  = .1E+01, 0.0, 0.0, 0.0, 0.0, 0.0, 0.0, 0.0, 0.0, 0.0,
VFACTR = .3E+01,
TIMEOO = 0.0, 0.0, 0.0, 0.0, 0.0, 0.0,
JKEEP  = 300,
XO     = .102E+04, .102E+04, 0.0, 0.0, 0.0, 0.0, 0.0, 0.0, 0.0, 0.0,
YO     = 0.0, .85E+02, 0.0, 0.0, 0.0, 0.0, 0.0, 0.0, 0.0, 0.0,
ZO     = .49E+03, .49E+03, 0.0, 0.0, 0.0, 0.0, 0.0, 0.0, 0.0, 0.0,
GO     = T,
$END
```

TABLE VI SOURCE RATES USED IN RETURN FLUX PREDICTIONS

REPORT NO. 11 **** RETURN FLUX ******

12/06/77 23.56.57.

CONTENTS: PHYSICAL CHARACTERISTICS OF SURFACE SOURCES AT TIME 0.HRS 3.MINS 0.SECS

SURFACE NUMBER	AREA (IN**2) (CM**2)	SECTION MATERIAL	MASS LOSS (GM/SEC) TEMP (DEG C)	SPECIES MASS LOSS RATES (GM/CM**2/SEC) OUTG1 O2	OUTG2 CO	H2O H2	N2 H	CO2 MMHNO3	EARLY DESORPTION	OUT GASSING
200	.20E+05 .13E+06	FUSLAG LRSI	.138E-04 54.	.11E-09 0.	0. 0.	0. 0.	0. 0.	0. 0.	0.	..06E-09
203	.33E+05 .21E+06	FUSLAG LRSI	.123E-04 37.	.59E-10 0.	0. 0.	0. 0.	0. 0.	0. 0.	0.	.585E-10
202	.33E+05 .21E+06	FUSLAG LRSI	.123E-04 37.	.59E-10 0.	0. 0.	0. 0.	0. 0.	0. 0.	0.	.585E-10
50	.26E+05 .17E+06	RADOOR TEFLON	.813E-05 33.	.49E-10 0.	0. 0.	0. 0.	0. 0.	0. 0.	0.	.492E-10
40	.26E+05 .17E+06	RADCOR TEFLON	.813E-05 33.	.49E-10 0.	0. 0.	0. 0.	0. 0.	0. 0.	0.	.492E-10
32	.12E+05 .79E+05	RADOOR TEFLON	.702E-05 50.	.89E-10 0.	0. 0.	0. 0.	0. 0.	0. 0.	0.	.892E-10
34	.12E+05 .79E+05	RADOOR TEFLON	.702E-05 50.	.89E-10 0.	0. 0.	0. 0.	0. 0.	0. 0.	0.	.892E-10
36	.12E+05 .79E+05	RADOOR TEFLON	.702E-05 50.	.89E-10 0.	0. 0.	0. 0.	0. 0.	0. 0.	0.	.892E-10
20	.12E+05 .79E+05	RADCOR TEFLON	.702E-05 50.	.89E-10 0.	0. 0.	0. 0.	0. 0.	0. 0.	0.	.892E-10
22	.12E+05 .79E+05	RADOOR TEFLON	.702E-05 50.	.89E-10 0.	0. 0.	0. 0.	0. 0.	0. 0.	0.	.892E-10
24	.12E+05 .79E+05	RADOOR TEFLON	.702E-05 50.	.89E-10 0.	0. 0.	0. 0.	0. 0.	0. 0.	0.	.892E-10
26	.12E+05 .79E+05	RADOOR TEFLON	.702E-05 50.	.89E-10 0.	0. 0.	0. 0.	0. 0.	0. 0.	0.	.892E-10

TABLE VI SOURCE RATES USED IN RETURN FLUX PREDICTIONS - continued

30	.12E+05	RADOOR	.702E-05	.89E-10	0.	0.	0.	0.		
	.79E+05	TEFLON	50.	0.	0.	0.	0.	0.	0.	.892E-10
110	.23E+05	WING	.691E-05	.46E-10	0.	0.	0.	0.		
	.15E+06	NOMEX	4.	0.	0.	0.	0.	0.	0.	.459E-10
140	.23E+05	WING	.691E-05	.46E-10	0.	0.	0.	0.		
	.15E+06	NOMEX	4.	0.	0.	0.	0.	0.	0.	.459E-10
64	.38E+05	OMS	.666E-05	.27E-10	0.	0.	0.	0.		
	.24E+06	LRSI	15.	0.	0.	0.	0.	0.	0.	.272E-10
44	.26E+05	RADOOR	.666E-05	.40E-10	0.	0.	0.	0.		
	.17E+06	TEFLON	27.	0.	0.	0.	0.	0.	0.	.403E-10
84	.38E+05	OMS	.662E-05	.27E-10	0.	0.	0.	0.		
	.24E+06	LRSI	15.	0.	0.	0.	0.	0.	0.	.272E-10
54	.26E+05	RADOOR	.633E-05	.39E-10	0.	0.	0.	0.		
	.17E+06	TEFLON	26.	0.	0.	0.	0.	0.	0.	.385E-10
161	.93E+04	CREW	.632E-05	.10E-09	0.	0.	0.	0.		
	.60E+05	LRSI	54.	0.	0.	0.	0.	0.	0.	..05E-09
316	.31E+05	FUSLAG	.601E-05	.30E-10	0.	0.	0.	0.		
	.20E+06	NOMEX	-8.	0.	0.	0.	0.	0.	0.	.301E-10
174	.21E+05	CREW	.597E-05	.45E-10	0.	0.	0.	0.		
	.13E+06	LRSI	29.	0.	0.	0.	0.	0.	0.	.447E-10
306	.31E+05	FUSLAG	.597E-05	.30E-10	0.	0.	0.	0.		
	.20E+06	NOMEX	-8.	0.	0.	0.	0.	0.	0.	.299E-10
112	.19E+05	WING	.574E-05	.45E-10	0.	0.	0.	0.		
	.13E+06	NOMEX	4.	0.	0.	0.	0.	0.	0.	.459E-10
142	.19E+05	WING	.574E-05	.46E-10	0.	0.	0.	0.		
	.13E+06	NOMEX	4.	0.	0.	0.	0.	0.	0.	.459E-10
107	.17E+05	ELEVON	.561E-05	.51E-10	0.	0.	0.	0.		
	.11E+06	NOMEX	7.	0.	0.	0.	0.	0.	0.	.505E-10
11	.33E+05	BAY	.527E-05	.25E-10	0.	0.	0.	0.		
	.21E+06	BLKHED	-7.	0.	0.	0.	0.	0.	0.	.250E-10
13	.33E+05	BAY	.527E-05	.25E-10	0.	0.	0.	0.		
	.21E+06	BLKHED	-7.	0.	0.	0.	0.	0.	0.	.250E-10

TABLE VI SOURCE RATES USED IN RETURN FLUX PREDICTIONS - continued

230	.26E+05	FUSLAG	.507E-05	.31E-10	0.	0.	0.	0.	0.	.305E-10
	.17E+06	LRSI	18.	0.	0.	0.	0.	0.		
166	.43E+04	CREW	.488E-05	.18E-09	0.	0.	0.	0.	0.	..78E-09
	.27E+05	LRSI	69.	0.	0.	0.	0.	0.		
165	.43E+04	CREW	.488E-05	.18E-09	0.	0.	0.	0.	0.	..78E-09
	.27E+05	LRSI	69.	0.	0.	0.	0.	0.		
307	.25E+05	FUSLAG	.476E-05	.30E-10	0.	0.	0.	0.	0.	.299E-10
	.16E+06	NOMEX	-8.	0.	0.	0.	0.	0.		
132	.30E+05	WING	.434E-05	.23E-10	0.	0.	0.	0.	0.	.227E-10
	.19E+06	NOMEX	-16.	0.	0.	0.	0.	0.		
102	.30E+05	WING	.434E-05	.23E-10	0.	0.	0.	0.	0.	.227E-10
	.19E+06	NOMEX	-16.	0.	0.	0.	0.	0.		
190	.10E+05	CREW	.410E-05	.62E-10	0.	0.	0.	0.	0.	.620E-10
	.66E+05	LRSI	39.	0.	0.	0.	0.	0.		
311	.27E+05	FUSLAG	.393E-05	.23E-10	0.	0.	0.	0.	0.	.229E-10
	.17E+06	LRSI	10.	0.	0.	0.	0.	0.		
315	.31E+05	FUSLAG	.377E-05	.19E-10	0.	0.	0.	0.	0.	..89E-10
	.20E+06	LRSI	4.	0.	0.	0.	0.	0.		
317	.25E+05	FUSLAG	.376E-05	.24E-10	0.	0.	0.	0.	0.	.235E-10
	.16E+06	NOMEX	-15.	0.	0.	0.	0.	0.		
305	.31E+05	FUSLAG	.371E-05	.19E-10	0.	0.	0.	0.	0.	..86E-10
	.20E+06	LRSI	4.	0.	0.	0.	0.	0.		
115	.19E+05	WING	.359E-05	.29E-10	0.	0.	0.	0.	0.	.288E-10
	.12E+06	LRSI	17.	0.	0.	0.	0.	0.		
145	.19E+05	WING	.359E-05	.29E-10	0.	0.	0.	0.	0.	.288E-10
	.12E+06	LRSI	17.	0.	0.	0.	0.	0.		
301	.27E+05	FUSLAG	.357E-05	.21E-10	0.	0.	0.	0.	0.	.208E-10
	.17E+06	LRSI	7.	0.	0.	0.	0.	0.		
163	.34E+04	CREW	.339E-05	.16E-09	0.	0.	0.	0.	0.	..56E-09
	.22E+05	LRSI	66.	0.	0.	0.	0.	0.		
164	.34E+04	CREW	.334E-05	.15E-09	0.	0.	0.	0.	0.	..53E-09
	.22E+05	LRSI	65.	0.	0.	0.	0.	0.		

TABLE VI SOURCE RATES USED IN RETURN FLUX PREDICTIONS - continued

241	.16E+05	FUSLAG	.322E-05	.31E-10	0.	0.	0.	0.		
	.11E+06	LRSI	18.	0.	0.	0.	0.	0.	0.	.305E-10
162	.93E+04	CREW	.317E-05	.53E-10	0.	0.	0.	0.		
	.60E+05	LRSI	34.	0.	0.	0.	0.	0.	0.	.526E-10
137	.91E+04	ELEVON	.298E-05	.51E-10	0.	0.	0.	0.		
	.59E+05	NOMEX	7.	0.	0.	0.	0.	0.	0.	.505E-10
134	.91E+04	WING	.202E-05	.34E-10	0.	0.	0.	0.		
	.59E+05	NOMEX	-4.	0.	0.	0.	0.	0.	0.	.344E-10
104	.91E+04	WING	.202E-05	.34E-10	0.	0.	0.	0.		
	.59E+05	NOMEX	-4.	0.	0.	0.	0.	0.	0.	.344E-10
240	.16E+05	FUSLAG	.196E-05	.19E-10	0.	0.	0.	0.		
	.11E+06	LRSI	4.	0.	0.	0.	0.	0.	0.	.185E-10
136	.65E+04	ELEVON	.192E-05	.46E-10	0.	0.	0.	0.		
	.42E+05	NOMEX	4.	0.	0.	0.	0.	0.	0.	.459E-10
106	.65E+04	ELEVON	.192E-05	.46E-10	0.	0.	0.	0.		
	.42E+05	NOMEX	4.	0.	0.	0.	0.	0.	0.	.459E-10
130	.64E+04	WING	.173E-05	.42E-10	0.	0.	0.	0.		
	.41E+05	NOMEX	2.	0.	0.	0.	0.	0.	0.	.422E-10
100	.64E+04	WING	.173E-05	.42E-10	0.	0.	0.	0.		
	.41E+05	NOMEX	2.	0.	0.	0.	0.	0.	0.	.422E-10
46	.26E+05	RADOOR	.163E-05	.98E-11	0.	0.	0.	0.		
	.17E+06	TEFLON	-14.	0.	0.	0.	0.	0.	0.	.985E-11
56	.25E+05	RADOOR	.159E-05	.98E-11	0.	0.	0.	0.		
	.16E+06	TEFLON	-14.	0.	0.	0.	0.	0.	0.	.985E-11
62	.79E+04	OMS	.138E-05	.27E-10	0.	0.	0.	0.		
	.51E+05	LRSI	15.	0.	0.	0.	0.	0.	0.	.272E-10
82	.78E+04	OMS	.137E-05	.27E-10	0.	0.	0.	0.		
	.50E+05	LRSI	15.	0.	0.	0.	0.	0.	0.	.272E-10
35	.12E+05	FUSLAG	.127E-05	.16E-10	0.	0.	0.	0.		
	.79E+05	LRSI	-0.	0.	0.	0.	0.	0.	0.	.161E-10

TABLE VI SOURCE RATES USED IN RETURN FLUX PREDICTIONS - continued

27	.12E+05 .79E+05	FUSLAG LRSI	.124E-05 -1.	.16E-10 0. 0. 0.	0. 0.	0. 0.	0. 0.	0.	..57E-10
31	.12E+05 .79E+05	FUSLAG LRSI	.107E-05 -5.	.14E-10 0. 0. 0.	0. 0.	0. 0.	0. 0.	0.	..36E-10
23	.12E+05 .79E+05	FUSLAG LRSI	.106E-05 -5.	.14E-10 0. 0. 0.	0. 0.	0. 0.	0. 0.	0.	..35E-10
380	.17E+05 .11E+06	TAIL LRSI	.985E-06 -17.	.90E-11 0. 0. 0.	0. 0.	0. 0.	0. 0.	0.	.902E-11
381	.17E+05 .11E+06	TAIL LRSI	.985E-06 -17.	.90E-11 0. 0. 0.	0. 0.	0. 0.	0. 0.	0.	.902E-11
459	.26E+04 .17E+05	ELEVCN NOMEX	.945E-06 10.	.56E-10 0. 0. 0.	0. 0.	0. 0.	0. 0.	0.	.557E-10
469	.26E+04 .17E+05	ELEVON NOMEX	.945E-06 10.	.56E-10 0. 0. 0.	0. 0.	0. 0.	0. 0.	0.	.557E-10
468	.24E+04 .15E+05	ELEVON NOMEX	.845E-06 10.	.56E-10 0. 0. 0.	0. 0.	0. 0.	0. 0.	0.	.557E-10
458	.24E+04 .15E+05	ELEVON NOMEX	.845E-06 10.	.56E-10 0. 0. 0.	0. 0.	0. 0.	0. 0.	0.	.557E-10
167	.13E+05 .81E+05	CREW HRSI	.828E-06 -14.	.10E-10 0. 0. 0.	0. 0.	0. 0.	0. 0.	0.	..02E-10
168	.13E+05 .81E+05	CREW HRSI	.812E-06 -15.	.10E-10 0. 0. 0.	0. 0.	0. 0.	0. 0.	0.	..00E-10
384	.14E+05 .90E+05	TAIL LRSI	.812E-06 -17.	.90E-11 0. 0. 0.	0. 0.	0. 0.	0. 0.	0.	.902E-11
385	.14E+05 .90E+05	TAIL LRSI	.812E-06 -17.	.90E-11 0. 0. 0.	0. 0.	0. 0.	0. 0.	0.	.902E-11
457	.21E-04 .13E+05	ELEVON NOMEX	.746E-06 10.	.56E-10 0. 0. 0.	0. 0.	0. 0.	0. 0.	0.	.557E-10
467	.21E+04 .13E+05	ELEVON NOMEX	.746E-06 10.	.56E-10 0. 0. 0.	0. 0.	0. 0.	0. 0.	0.	.557E-10

TABLE VI SOURCE RATES USED IN RETURN FLUX PREDICTIONS - continued

42	.26E+05	RADOOR	.727E-06	.44E-11	0.	0.	0.	0.		
	.17E+06	TEFLON	-37.	0.	0.	0.	0.	0.	0.	.441E-11
52	.26E+05	RADOOR	.727E-06	.44E-11	0.	0.	0.	0.		
	.17E+06	TEFLON	-37.	0.	0.	0.	0.	0.	0.	.441E-11
117	.57E+04	WING	.716E-06	.20E-10	0.	0.	0.	0.		
	.36E+05	HRSI	5.	0.	0.	0.	0.	0.	0.	..96E-10
147	.57E+04	WING	.716E-06	.20E-10	0.	0.	0.	0.		
	.36E+05	HRSI	5.	0.	0.	0.	0.	0.	0.	..96E-10
3	.27E+05	BAY	.661E-06	.38E-11	0.	0.	0.	0.		
	.17E+06	LINER	12.	0.	0.	0.	0.	0.	0.	.385E-11
4	.27E+05	BAY	.661E-06	.38E-11	0.	0.	0.	0.		
	.17E+06	LINER	12.	0.	0.	0.	0.	0.	0.	.385E-11
5	.27E+05	BAY	.661E-06	.38E-11	0.	0.	0.	0.		
	.17E+06	LINER	12.	0.	0.	0.	0.	0.	0.	.385E-11
6	.27E+05	BAY	.661E-06	.38E-11	0.	0.	0.	0.		
	.17E+06	LINER	12.	0.	0.	0.	0.	0.	0.	.385E-11
7	.27E+05	BAY	.661E-06	.38E-11	0.	0.	0.	0.		
	.17E+06	LINER	12.	0.	0.	0.	0.	0.	0.	.385E-11
8	.27E+05	BAY	.661E-06	.38E-11	0.	0.	0.	0.		
	.17E+06	LINER	12.	0.	0.	0.	0.	0.	0.	.385E-11
1	.27E+05	BAY	.661E-06	.38E-11	0.	0.	0.	0.		
	.17E+06	LINER	12.	0.	0.	0.	0.	0.	0.	.385E-11
2	.27E+05	BAY	.661E-06	.38E-11	0.	0.	0.	0.		
	.17E+06	LINER	12.	0.	0.	0.	0.	0.	0.	.385E-11
466	.18E+04	ELEVON	.646E-06	.56E-10	0.	0.	0.	0.		
	.12E+05	NOMEX	10.	0.	0.	0.	0.	0.	0.	.557E-10
456	.18E+04	ELEVON	.646E-06	.56E-10	0.	0.	0.	0.		
	.12E+05	NOMEX	10.	0.	0.	0.	0.	0.	0.	.557E-10
455	.15E+04	ELEVON	.547E-06	.56E-10	0.	0.	0.	0.		
	.98E+04	NOMEX	10.	0.	0.	0.	0.	0.	0.	.557E-10
465	.15E+04	ELEVON	.547E-06	.56E-10	0.	0.	0.	0.		
	.98E+04	NOMEX	10.	0.	0.	0.	0.	0.	0.	.557E-10

TABLE VI SOURCE RATES USED IN RETURN FLUX PREDICTIONS - continued

382	.88E+04	TAIL	.514E-06	.90E-11	0.	0.	0.	0.			
	.57E+05	LRSI	-17.	0.	0.	0.	0.	0.	0.	.902E-11	,
383	.88E+04	TAIL	.514E-06	.90E-11	0.	0.	0.	0.			
	.57E+05	LRSI	-17.	0.	0.	0.	0.	0.	0.	.902E-11	
464	.12E+04	ELEVON	.448E-06	.56E-10	0.	0.	0.	0.			
	.80E+04	NOMEX	10.	0.	0.	0.	0.	0.	0.	.557E-10	
454	.12E+04	ELEVON	.448E-06	.56E-10	0.	0.	0.	0.			
	.80E+04	NOMEX	10.	0.	0.	0.	0.	0.	0.	.557E-10	
119	.33E+04	WING	.402E-06	.19E-10	0.	0.	0.	0.			
	.21E+05	LRSI	4.	0.	0.	0.	0.	0.	0.	..89E-10	
149	.33E+04	WING	.397E-06	.19E-10	0.	0.	0.	0.			
	.21E+05	LRSI	4.	0.	0.	0.	0.	0.	0.	..8GE-10	
386	.61E+04	TAIL	.356E-06	.90E-11	0.	0.	0.	0.			
	.39E+05	LRSI	-17.	0.	0.	0.	0.	0.	0.	.902E-11	
387	.61E+04	TAIL	.356E-06	.90E-11	0.	0.	0.	0.			
	.39E+05	LRSI	-17.	0.	0.	0.	0.	0.	0.	.902E-11	
67	.20E+04	OMS	.356E-06	.27E-10	0.	0.	0.	0.			
	.13E+05	LRSI	15.	0.	0.	0.	0.	0.	0.	.272E-10	
97	.20E+04	OMS	.356E-06	.27E-10	0.	0.	0.	0.			
	.13E+05	LRSI	15.	0.	0.	0.	0.	0.	0.	.272E-10	
25	.12E+05	FUSLAG	.354E-06	.45E-11	0.	0.	0.	0.			
	.79E+05	LRSI	-37.	0.	0.	0.	0.	0.	0.	.449E-11	
37	.12E+05	FUSLAG	.354E-06	.45E-11	0.	0.	0.	0.			
	.79E+05	LRSI	-37.	0.	0.	0.	0.	0.	0.	.449E-11	
86	.20E+04	OMS	.349E-06	.27E-10	0.	0.	0.	0.			
	.13E+05	LRSI	15.	0.	0.	0.	0.	0.	0.	.272E-10	
66	.20E+04	OMS	.349E-06	.27E-10	0.	0.	0.	0.			
	.13E+05	LRSI	15.	0.	0.	0.	0.	0.	0.	.272E-10	
463	.97E+03	ELEVON	.348E-06	.56E-10	0.	0.	0.	0.			
	.63E+04	NOMEX	10.	0.	0.	0.	0.	0.	0.	.557E-10	
453	.96E+03	ELEVON	.345E-06	.56E-10	0.	0.	0.	0.			
	.62E+04	NOMEX	10.	0.	0.	0.	0.	0.	0.	.557E-10	

TABLE VI SOURCE RATES USED IN RETURN FLUX PREDICTIONS - continued

148	.25E+04	WING	.318E-06	.20E-10	0.	0.	0.	0.		
	.16E+05	MRSI	5.	0.	0.	0.	0.	0.	0.	..96E-10
118	.25E+04	WING	.318E-06	.20E-10	0.	0.	0.	0.		
	.16E+05	MRSI	5.	0.	0.	0.	0.	0.	0.	..96E-10
462	.69E+03	ELEVON	.249E-06	.56E-10	0.	0.	0.	0.		
	.45E+04	NOWEX	10.	0.	0.	0.	0.	0.	0.	.557E-10
452	.69E+03	ELEVON	.249E-06	.56E-10	0.	0.	0.	0.		
	.45E+04	NOWEX	10.	0.	0.	0.	0.	0.	0.	.557E-10
72	.14E+04	OMS	.247E-06	.27E-10	0.	0.	0.	0.		
	.91E+04	LRSI	15.	0.	0.	0.	0.	0.	0.	.272E-10
92	.14E+04	OMS	.247E-06	.27E-10	0.	0.	0.	0.		
	.91E+04	LRSI	15.	0.	0.	0.	0.	0.	0.	.272E-10
41	.26E+05	FUSLAG	.232E-06	.14E-11	0.	0.	0.	0.		
	.17E+06	LRSI	-71.	0.	0.	0.	0.	0.	0.	..41E-11
45	.26E+05	FUSLAG	.232E-06	.14E-11	0.	0.	0.	0.		
	.17E+06	LRSI	-71.	0.	0.	0.	0.	0.	0.	..41E-11
74	.13E+04	OMS	.230E-06	.27E-10	0.	0.	0.	0.		
	.85E+04	LRSI	15.	0.	0.	0.	0.	0.	0.	.272E-10
94	.13E+04	OMS	.230E-06	.27E-10	0.	0.	0.	0.		
	.85E+04	LRSI	15.	0.	0.	0.	0.	0.	0.	.272E-10
399	.38E+04	TAIL	.227E-06	.92E-11	0.	0.	0.	0.		
	.25E+05	MRSI	-17.	0.	0.	0.	0.	0.	0.	.920E-11
55	.25E+05	FUSLAG	.227E-06	.14E-11	0.	0.	0.	0.		
	.16E+06	LRSI	-71.	0.	0.	0.	0.	0.	0.	..41E-11
51	.25E+05	FUSLAG	.227E-06	.14E-11	0.	0.	0.	0.		
	.16E+06	LRSI	-71.	0.	0.	0.	0.	0.	0.	..41E-11
250	.20E+05	FUSLAG	.206E-06	.16E-11	0.	0.	0.	0.		
	.13E+06	LRSI	-67.	0.	0.	0.	0.	0.	0.	..63E-11
80	.11E+04	OMS	.201E-06	.27E-10	0.	0.	0.	0.		
	.74E+04	LRSI	15.	0.	0.	0.	0.	0.	0.	.272E-10
60	.11E+04	OMS	.201E-06	.27E-10	0.	0.	0.	0.		
	.74E+04	LRSI	15.	0.	0.	0.	0.	0.	0.	.272E-10

TABLE VI SOURCE RATES USED IN RETURN FLUX PREDICTIONS - continued

43	.26E+05	FUSLAG	.190E-06	.12E-11	0.	0.	0.	0.		
	.17E+06	LRSI	-77.	0.	0.	0.	0.	0.	0.	..15E-11
47	.26E+05	FUSLAG	.190E-06	.12E-11	0.	0.	0.	0.		
	.17E+06	LRSI	-77.	0.	0.	0.	0.	0.	0.	..15E-11
53	.25E+05	FUSLAG	.186E-06	.12E-11	0.	0.	0.	0.		
	.16E+06	LRSI	-77.	0.	0.	0.	0.	0.	0.	..15E-11
57	.25E+05	FUSLAG	.186E-06	.12E-11	0.	0.	0.	0.		
	.16E+06	LRSI	-77.	0.	0.	0.	0.	0.	0.	..15E-11
21	.12E+05	FUSLAG	.185E-06	.24E-11	0.	0.	0.	0.		
	.79E+05	LRSI	-56.	0.	0.	0.	0.	0.	0.	.235E-11
33	.12E+05	FUSLAG	.181E-06	.23E-11	0.	0.	0.	0.		
	.79E+05	LRSI	-57.	0.	0.	0.	0.	0.	0.	.230E-11
393	.31E+04	TAIL	.179E-06	.90E-11	0.	0.	0.	0.		
	.20E+05	LRSI	-17.	0.	0.	0.	0.	0.	0.	.902E-11
392	.31E+04	TAIL	.179E-06	.90E-11	0.	0.	0.	0.		
	.20E+05	LRSI	-17.	0.	0.	0.	0.	0.	0.	.902E-11
389	.27E+04	TAIL	.160E-06	.90E-11	0.	0.	0.	0.		
	.18E+05	LRSI	-17.	0.	0.	0.	0.	0.	0.	.902E-11
388	.27E+04	TAIL	.160E-06	.90E-11	0.	0.	0.	0.		
	.18E+05	LRSI	-17.	0.	0.	0.	0.	0.	0.	.902E-11
90	.90E+03	OMS	.157E-06	.27E-10	0.	0.	0.	0.		
	.58E+04	LRSI	15.	0.	0.	0.	0.	0.	0.	.272E-10
70	.90E+03	OMS	.157E-06	.27E-10	0.	0.	0.	0.		
	.58E+04	LRSI	15.	0.	0.	0.	0.	0.	0.	.272E-10
461	.42E+03	ELEVON	.149E-06	.56E-10	0.	0.	0.	0.		
	.27E+04	NOMEX	10.	0.	0.	0.	0.	0.	0.	.557E-10
451	.42E+03	ELEVON	.149E-06	.56E-10	0.	0.	0.	0.		
	.27E+04	NOMEX	10.	0.	0.	0.	0.	0.	0.	.557E-10
175	.10E+05	CREW	.149E-06	.23E-11	0.	0.	0.	0.		
	.65E+05	LRSI	-57.	0.	0.	0.	0.	0.	0.	.227E-11

TABLE VI SOURCE RATES USED IN RETURN FLUX PREDICTIONS - continued

177	.10E+05	CREW	.145E-06	.22E-11	0.	0.	0.	0.		
	.65E+05	LRSI	-58.	0.	0.	0.	0.	0.	0.	.221E-11
96	.72E+03	OMS	.125E-06	.27E-10	0.	0.	0.	0.		
	.46E+04	LRSI	15.	0.	0.	0.	0.	0.	0.	.272E-10
76	.72E+03	OMS	.125E-06	.27E-10	0.	0.	0.	0.		
	.46E+04	LRSI	15.	0.	0.	0.	0.	0.	0.	.272E-10
97	.60E+03	OMS	.105E-06	.27E-10	0.	0.	0.	0.		
	.39E+04	LRSI	15.	0.	0.	0.	0.	0.	0.	.272E-10
170	.96E+04	CREW	.105E-06	.17E-11	0.	0.	0.	0.		
	.62E+05	HRSI	-66.	0.	0.	0.	0.	0.	0.	..70E-11
77	.60E+03	OMS	.105E-06	.27E-10	0.	0.	0.	0.		
	.39E+04	LRSI	15.	0.	0.	0.	0.	0.	0.	.272E-10
169	.96E+04	CREW	.105E-06	.17E-11	0.	0.	0.	0.		
	.62E+05	HRSI	-66.	0.	0.	0.	0.	0.	0.	..69E-11
425	.13E+04	FUSLAG	.104E-06	.12E-10	0.	0.	0.	0.		
	.85E+04	LRSI	-8.	0.	0.	0.	0.	0.	0.	..23E-10
420	.13E+04	FUSLAG	.104E-06	.12E-10	0.	0.	0.	0.		
	.85E+04	LRSI	-8.	0.	0.	0.	0.	0.	0.	..23E-10
440	.34E+04	BAY	.855E-07	.38E-11	0.	0.	0.	0.		
	.22E+05	LINER	12.	0.	0.	0.	0.	0.	0.	.385E-11
441	.34E+04	BAY	.855E-07	.38E-11	0.	0.	0.	0.		
	.22E+05	LINER	12.	0.	0.	0.	0.	0.	0.	.385E-11
442	.34E+04	BAY	.855E-07	.38E-11	0.	0.	0.	0.		
	.22E+05	LINER	12.	0.	0.	0.	0.	0.	0.	.385E-11
443	.34E+04	BAY	.855E-07	.38E-11	0.	0.	0.	0.		
	.22E+05	LINER	12.	0.	0.	0.	0.	0.	0.	.385E-11
445	.34E+04	BAY	.855E-07	.38E-11	0.	0.	0.	0.		
	.22E+05	LINER	12.	0.	0.	0.	0.	0.	0.	.385E-11
446	.34E+04	BAY	.855E-07	.38E-11	0.	0.	0.	0.		
	.22E+05	LINER	12.	0.	0.	0.	0.	0.	0.	.385E-11

TABLE VI SOURCE RATES USED IN RETURN FLUX PREDICTIONS - continued

447	.34E+04	BAY	.855E-07	.38E-11	0.	0.	0.	0.		
	.22E+05	LINER	12.	0.	0.	0.	0.	0.	0.	.385E-11
448	.34E+04	BAY	.855E-07	.38E-11	0.	0.	0.	0.		
	.22E+05	LINER	12.	0.	0.	0.	0.	0.	0.	.385E-11
68	.42E+03	OMS	.728E-07	.27E-10	0.	0.	0.	0.		
	.27E+04	LRSI	15.	0.	0.	0.	0.	0.	0.	.272E-10
88	.42E+03	OMS	.728E-07	.27E-10	0.	0.	0.	0.		
	.27E+04	LRSI	15.	0.	0.	0.	0.	0.	0.	.272E-10
391	.12E+04	TAIL	.675E-07	.90E-11	0.	0.	0.	0.		
	.75E+04	LRSI	-17.	0.	0.	0.	0.	0.	0.	.902E-11
390	.12E+04	TAIL	.675E-07	.90E-11	0.	0.	0.	0.		
	.75E+04	LRSI	-17.	0.	0.	0.	0.	0.	0.	.902E-11
450	.14E+03	ELEVON	.496E-07	.56E-10	0.	0.	0.	0.		
	.89E+03	NOSEX	10.	0.	0.	0.	0.	0.	0.	.557E-10
460	.14E+03	ELEVON	.496E-07	.56E-10	0.	0.	0.	0.		
	.89E+03	NOSEX	10.	0.	0.	0.	0.	0.	0.	.557E-10
172	.37E+04	CREW	.317E-07	.13E-11	0.	0.	0.	0.		
	.24E+05	HRSI	-73.	0.	0.	0.	0.	0.	0.	..33E-11
171	.37E+04	CREW	.315E-07	.13E-11	0.	0.	0.	0.		
	.24E+05	HRSI	-73.	0.	0.	0.	0.	0.	0.	..32E-11
160	.72E+04	CREW	.315E-08	.68E-13	0.	0.	0.	0.		
	.46E+05	RCC	22.	0.	0.	0.	0.	0.	0.	.679E-13
122	.31E+04	WING	.761E-09	.38E-13	0.	0.	0.	0.		
	.20E+05	RCC	5.	0.	0.	0.	0.	0.	0.	.378E-13

TABLE VI SOURCE RATES USED IN RETURN FLUX PREDICTIONS - concluded

152	.31E+04	WING	.761E-09		.38E-13	0.	0.	0.	0.		
	.20E+05	RCC		5.	0.	0.	0.	0.	0.	0.	.378E-13
151	.23E+04	WING	.549E-09		.38E-13	0.	0.	0.	0.		
	.15E+05	RCC		5.	0.	0.	0.	0.	0.	0.	.378E-13
121	.23E+04	WING	.549E-09		.38E-13	0.	0.	0.	0.		
	.15E+05	RCC		5.	0.	0.	0.	0.	0.	0.	.378E-13
184	.14E+04	CREW	0.		0.	0.	0.	0.	0.		
	.92E+04	WINDOW		15.	0.	0.	0.	0.	0.	0.	0.
185	.14E+04	CREW	0.		0.	0.	0.	0.	0.		
	.92E+04	WINDOW		21.	0.	0.	0.	0.	0.	0.	0.
180	.14E+04	CREW	0.		0.	0.	0.	0.	0.		
	.92E+04	WINDOW		21.	0.	0.	0.	0.	0.	0.	0.
181	.14E+04	CREW	0.		0.	0.	0.	0.	0.		
	.92E+04	WINDOW		15.	0.	0.	0.	0.	0.	0.	0.
182	.14E+04	CREW	0.		0.	0.	0.	0.	0.		
	.92E+04	WINDOW		-40.	0.	0.	0.	0.	0.	0.	0.
183	.14E+04	CREW	0.		0.	0.	0.	0.	0.		
	.92E+04	WINDOW		24.	0.	0.	0.	0.	0.	0.	0.
TOTALS	.20E+07		.337E-03								
	.13E+08										
AVERAGE					.26E-10	0.	0.	0.	0.	0.	.262E-10
					0.	0.	0.	0.	0.		

TABLE VII RETURN FLUX RATES

REPORT NO. 43 **** RETURN FLUX ******

12/07/77 00.13.35.

CONTENTS: SUMMARY RETURN FLUX AT 300.0 KM ALTITUDE

CRITICAL SURFACE NO. = 1111
FIELD-OF-VIEW (SR) = 2.962

*** LISTED BY MATERIAL TYPE ***

SECTION SUMMARY	SPECIES RETURN FLUX (MOLECULES/CM**2) OUTG1 / O2	OUTG2 / CO	H2O / H2	N2 / H	CO2 / MMHNO3	EARLY DESORPTION (GM/CM**2) (MOLECULES/CM**2)	OUT GASSING	TOTAL	% OF TOTAL
LINER	.76E+10	0.	0.	0.	0.	0.	.13E-1.	.13E-11	
	0.	0.	0.	0.	0.	0.	.76E+10	.76E+10	3.5
TEFLON	.14E+12	0.	0.	0.	0.	0.	.23E-10	.23E-10	
	0.	0.	0.	0.	0.	0.	.14E+12	.14E+12	63.8
NOMEX	.26E+11	0.	0.	0.	0.	0.	.44E-1.	.44E-11	
	0.	0.	0.	0.	0.	0.	.26E+1.	.26E+11	11.9
LRSI	.32E+11	0.	0.	0.	0.	0.	.53E-1.	.53E-11	
	0.	0.	0.	0.	0.	0.	.32E+1.	.32E+11	14.4
HRSI	.19E+10	0.	0.	0.	0.	0.	.32E-12	.32E-12	
	0.	0.	0.	0.	0.	0.	.19E+10	.19E+10	.9
RCC	.19E+07	0.	0.	0.	0.	0.	.31E-15	.31E-15	
	0.	0.	0.	0.	0.	0.	.19E+07	.19E+07	.0
BLKHED	.12E+11	0.	0.	0.	0.	0.	.20E-1.	.20E-11	
	0.	0.	0.	0.	0.	0.	.12E+1.	.12E+11	5.5
TOTAL	.22E+12	0.	0.	0.	0.	0.	.36E-10	.36E-10	
	0.	0.	0.	0.	0.	0.	.22E+12	.22E+12	100.0

and -12 to -18°C receivers. This approach for these Orbiter sources is consistent with the SPACE program logic.*

In summary, the deposition rate is 2.49×10^{-11} g·cm^{-2}·s^{-1} for the IUS/DSP/radiator return flux and 3.9×10^{-12} g·cm^{-2}·s^{-1} for the remainder of the Orbiter. The net deposition after the two hour exposure time is 2.07×10^{-7} g·cm^{-2}·s^{-1} or 21Å thickness for a unit density deposit. This is calculated from D = M/V where

D = density,

M = mass and

V = volume.

The above analysis corresponds to a first flight Orbiter. Because the radiator surfaces will be warmer than most surfaces during a mission, it is conceivable that the mass loss rate will be near 1×10^{-11} g·cm^{-2}·s^{-1} after an initial mission and will consist primarily of VCM material. This behavior is indicated in Figure 7 which shows the mass loss rate is greatly reduced after 24 hours at temperatures near 48°C which are the temperatures anticipated for the radiators during on-orbit conditions. This would reduce the deposition flux to 8.94×10^{-12} g·cm^{-2}·s^{-1} or a total deposit of 6Å after the 7200 second exposure.

The return flux deposition values for outgassing sources are shown in Table III.

4.2.3 Engine Return Flux - The VCS engines are required for attitude control. It was established that the engines will not be required to be fired during the deployment maneuvers since the drift rate of the Orbiter is within acceptable limits. Therefore, the only time period during which the attitude control engines can contaminate the DSP surfaces is by the return flux mechanism during the in bay-doors open period while maintaining attitude control. Figure 10 shows the engine location and nomenclature. The engine, total firing time and return flux contribution are shown in Table VIII at the fixed attitude

* Users Manual, "Shuttle/Payload Contamination Evaluation Program" MCR-77-106, April 1977.

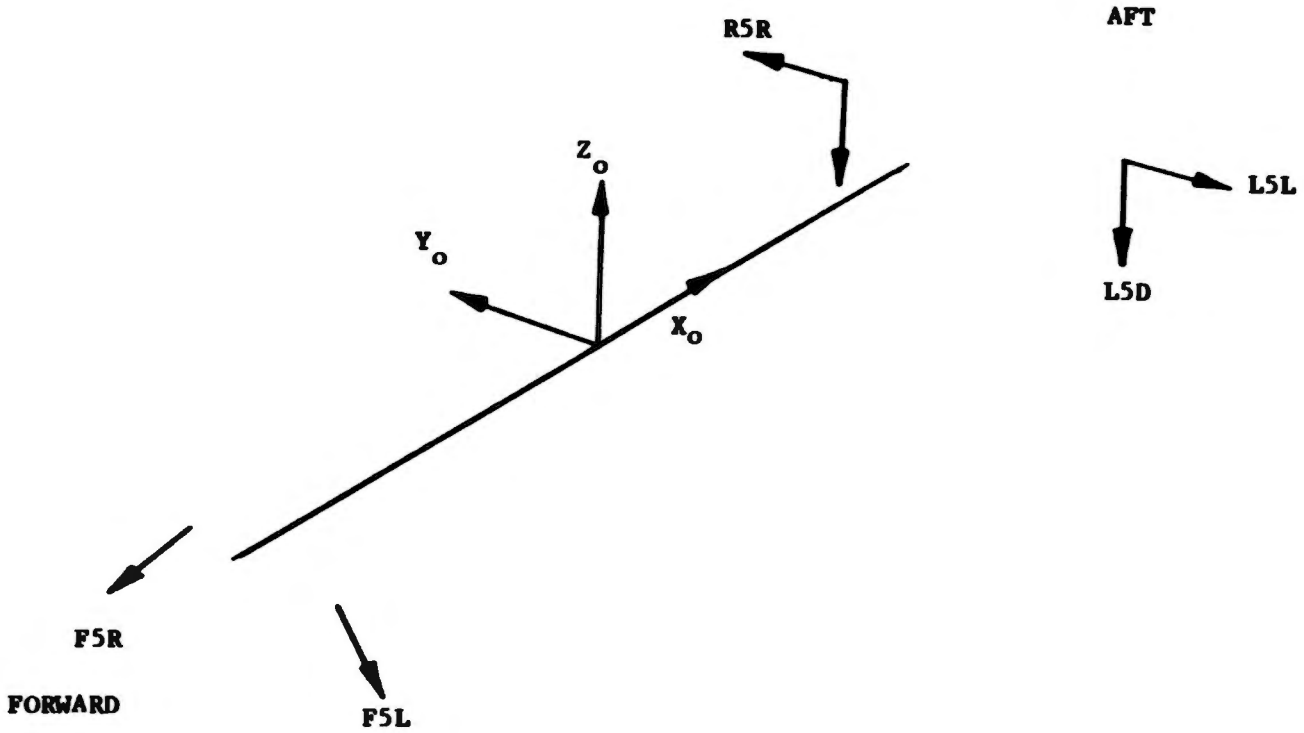

Figure 10 VCS Engine Nomenclature

of the mission. The engines and firing times resulted from an evaluation of altitude and attitude and resulting engine requirements by the mission and planning section at NASA-JSC.

TABLE VIII VCS ENGINE FIRING TIME AND RETURN FLUX CONTRIBUTION

Engine	On Time s	Return Flux Rate $g \cdot cm^{-2} \cdot s^{-1}$	Total Return Flux $g \cdot cm^{-2}$
F5L	6.32	4.75×10^{-10}	3.0×10^{-9}
F5R	6.72	4.75×10^{-10}	3.19×10^{-9}
L5L	0.68	1.36×10^{-9}	9.25×10^{-10}
L5D	1.24	9.05×10^{-11}	1.12×10^{-10}
R5D	1.08	9.05×10^{-11}	9.77×10^{-11}
R5R	0.96	1.36×10^{-9}	1.31×10^{-9}
		TOTAL	8.63×10^{-9}

Only the engine effluents that contribute directly to the column densities have condensible fractions in them capable of being scattered to surfaces in the payload bay. The fraction that is reflected off of the wings deposits the condensibles on the wing surfaces and, therefore, does not contribute to the column densities. The return flux values in Table VIII reflect only a small fraction (0.002) of the total engine effluent that is capable of condensing at DSP temperatures. This fraction is the $MMH\text{-}HNO_3$ that has been observed in testing. The results show that less than one angstrom (8.63×10^{-9} $g \cdot cm^{-2}$ = 0.86Å) of deposits occur on surfaces facing out of the bay normal to the Z axis. The same altitude and attitude were used for the engine return flux as for the outgassing return flux in the previous section.

4.3 Deployment - The deployment scheme is shown in Figure 5. The deposition from Orbiter surfaces during this period was less than an angstrom in all cases. This was primarily due to the short exposure duration at each deployment position. The deposition was calculated by summing the products of the source outgassing rate, the viewfactor between

the source and receiver and the condensation coefficient. The resulting deposition on the critical DSP surfaces is shown in Table III. A basic separation maneuver is performed at the last position by the Shuttle Orbiter forward facing nose location attitude control engines. Because of the relative location of the DSP surfaces and the engines, no net deposition results. The return flux on surfaces during deployment can be approximated by multiplying the in bay return flux rate by the exposure time at the different deployment positions. This would be a maximum case and results in only an angstrom or less of deposit.

4.4 Off Nominal - The off nominal periods evaluated were the 4.5 hours (nominal one hour) in bay-door closed and 24 hours (nominal 2 hours) in bay-doors open. For the in bay-doors closed case, the deposition would be 18Å for the baseline case assuming the mass loss rates are linear with time. The in bay-doors open values for a 24 hour exposure would be a maximum of 72Å for surfaces facing out of the bay normal to the Z axis when referring to Table III and assuming the rates are linear. The additional off nominal condition that was investigated was to vary the velocity vector orientation of the attitude and, thereby, change the return flux magnitudes. The nominal case and the variations analyzed are shown in Figure 11. The results indicate that by changing the velocity vector orientation so that it is 120 degrees with respect to the Z axis, the return flux can be reduced by a factor of three. If this were done for the 24 hour off nominal, in bay-doors open case, the deposition could be reduced from 72Å to approximately 24Å.

4.5 Representative Payload - A six sided box was used as a representative payload to determine relative flux levels from the Shuttle Orbiter and IUS during periods in the bay and during deployment. These relative flux levels will indicate the potentially most susceptible surfaces on a payload.

Figure 12 shows the position of the box (1.22 meters square on a side) relative to the IUS, the in bay position and the two deployment positions at 3.66 and 7.62 meters out of the bay. The node numbers of the box are also designated in the figure for correlation to the results shown in Table IX.

NOMINAL

RF = 3.9×10^{-11} g·cm^{-2}·s^{-1}

VARIATIONS

RF = 7.4×10^{-11} g·cm^{-2}·s^{-1} RF = 1.3×10^{-11} g·cm^{-2}·s^{-1}

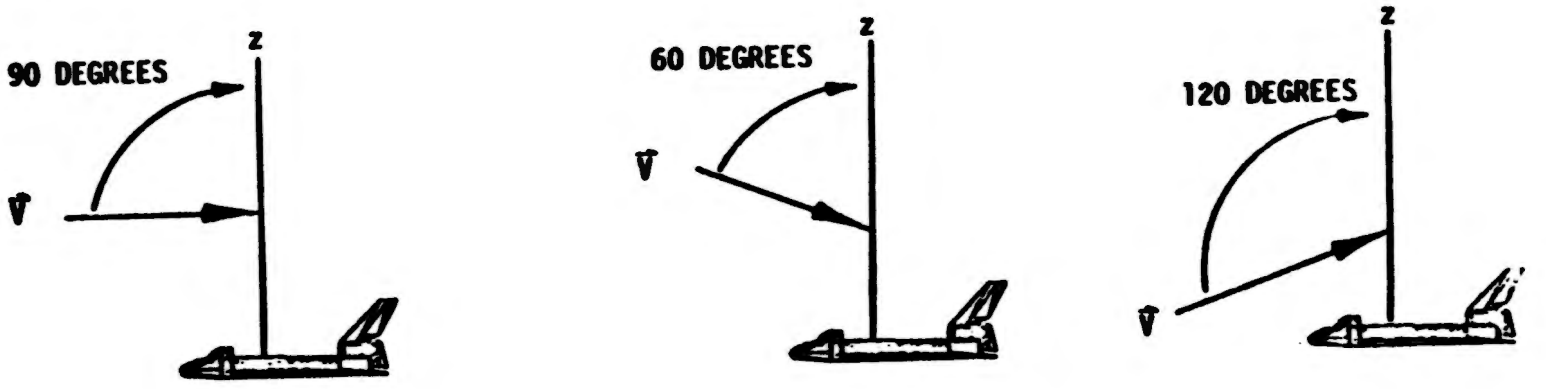

Figure 11 Velocity Vector Influence on Return Flux

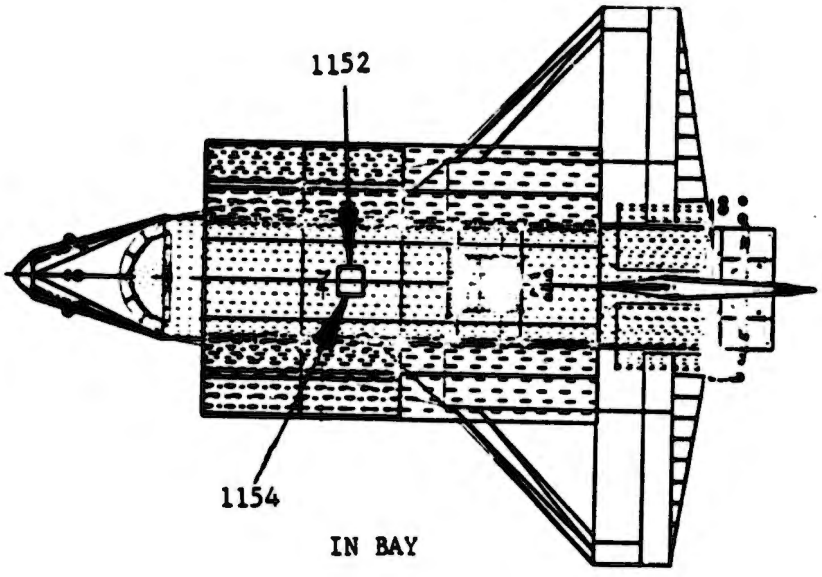

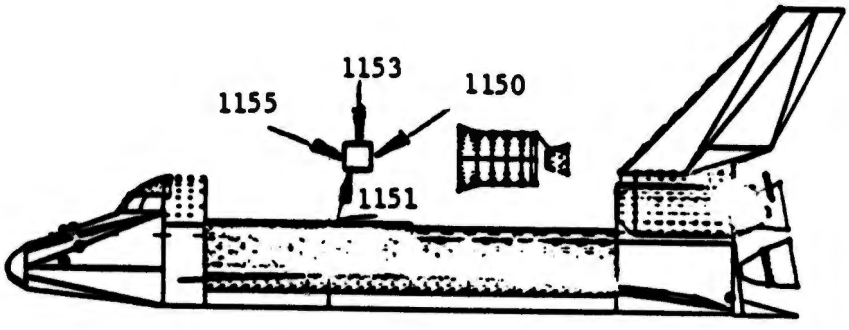

3.66 Meter(12 FOOT) DEPLOYMENT

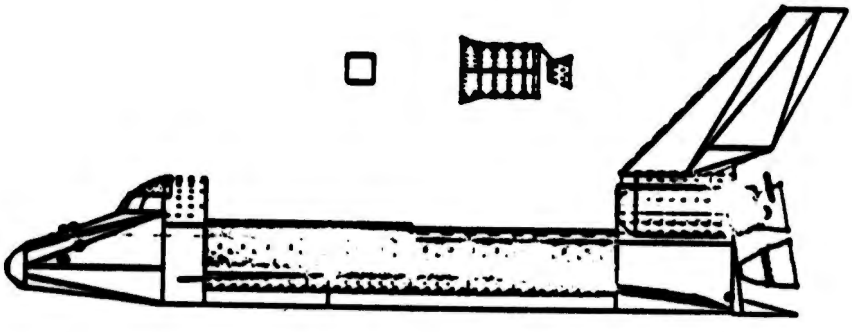

7.62 Meter(25 FOOT) DEPLOYMENT

Figure 12 Representative Payload Description and Location

TABLE IX DIRECT FLUXES, $g \cdot cm^{-2} \cdot s^{-1}$, ON REPRESENTATIVE PAYLOAD SURFACES

Surface	In Bay	3.66 Meters (12 feet)	7.62 Meters (25 feet)
1150 (AFT)	0.5×10^{-12}	0.95×10^{-12}	0.97×10^{-11}
1151 (DOWN)	0.65×10^{-12}	0.32×10^{-11}	0.34×10^{-10}
1152 (Y STARBOARD)	0.94×10^{-12}	0.24×10^{-11}	0.98×10^{-12}
*1153 (UP)	0.19×10^{-13}	0.0	0.0
1154 (Y PORT)	0.94×10^{-12}	0.24×10^{-11}	0.98×10^{-12}
1155 (FWD)	0.55×10^{-12}	0.37×10^{-11}	0.18×10^{-11}

* Return flux could be as high as 3.6×10^{-11} $g \cdot cm^{-2} \cdot s^{-1}$ for the upward facing surface while in the bay for the attitude used in this study. The return flux is a function of attitude and altitude and will vary for different missions.

The Orbiter temperatures used for the IUS/DSP study during in bay-doors open and deployment were used for this analysis. The results indicate that the Y facing surfaces receive the highest direct flux while in the bay. Not included here is the influence of return flux which would be highest on the Z (upward) facing surface. The magnitude of the return flux will be strongly dependent on the temperatures of the Orbiter, the orbital altitude and the relation of the velocity vector with respect to the payload bay.

From Table IX, it is shown that at the 3.66 meter deployment position the down facing and forward facing surfaces receive the highest flux. At the 7.62 meter deployment position, the down facing surface receives the highest flux. Both the aft and down facing surfaces have an increase in flux out to 7.62 meter while the others increase and then decrease during deployment except for node 1153 which views up.

The sources considered for the representative payload were the payload bay area, including the IUS and all external Shuttle Orbiter surfaces.

4.6 Results Summary - Table X summarizes the baseline deposition predictions for the fifteen critical DSP surfaces. The results include the reduction in VCM available by thermal vacuum testing of payload components and previous flight exposure of Shuttle Orbiter surfaces. The values in Table X are considered as a realistic prediction for the DSP spacecraft.

5.0 CONCLUSIONS

The following conclusions are a result of this study on the deposition levels predicted for DSP critical surfaces.

- The total pressure of gases in the payload bay during the doors closed period is 8×10^{-4} Torr.
- The mass input of VCM material into the payload bay during the door closed case is 2.17×10^{-5} $g \cdot s^{-1}$ or equivalently 3.69×10^{-3} $Torr \cdot l \cdot s^{-1}$.
- Previous flight exposure and thermal vacuum testing of nonmetallics significantly reduces VCM content and VCM mass loss rate.
- Deposition on all DSP surfaces during in bay-doors closed periods is 4Å for the one hour exposure time.
- Maximum values of return flux from outgassing sources on upward (Z facing) surfaces is 6Å for the two hour in bay-doors open exposure time.
- Direct flux from bay surfaces during the period in bay-doors open is less than one angstrom.
- Return flux from attitude control engines is less than one angstrom during the in bay-doors open period.
- Deposition during deployment is less than one angstrom on all DSP critical surfaces.
- Varying the angle of attack (velocity vector orientation changes) can significantly reduce return flux levels.

TABLE X SUMMARY-DEPOSITION

Node Number	Description	In Bay-Doors Closed (3600 s)	In Bay Doors Open (7200 s)			Station 1 (69.5 s)	Station 2 (193 s)	Station 3 (387.5 s)	Station 4 (193 s)	Station 5 (74 s)	Total Base-line Mission	Total with Off Nominal Doors Closed 4.5 Hours	Total with Off Nominal Doors Open 24 Hours
DSP	Surface Nomenclature	† Diffuse Flux	Direct Flux Å	* Return Flux Å Out-gassing	VCS	** Direct Flux Å	** Direct Flux Å	** Direct Flux Å	** Direct Flux Å	** Direct Flux Å	Å	Å	Å
1110	Solar Arrays	4	.045	6	<1	____	.0053	.034	.012	.0085	10.1	24.1	76.1
1111	Solar Arrays	4	.032	4	<1	.0042	.016	.02	.012	.0023	8.1	22.1	55.1
1112	Solar Arrays	4	.031	0		.0041	.0093	.0057	____	____	4.05	18.05	4.05
1113	Solar Arrays	4	.032	4	<1	.0042	.0028	.00011	.012	.0023	8.1	22.1	55.1
1153	OSR	4	.00017	6	<1	____	.000031	.0042	.0022	.001	10.1	24.1	76.1
1157	OSR	4	.043	0	0	.00087	.0024	.0045	.0017	.00022	4.05	18.05	4.05
1161	OSR	4	.017	0	0	.0012	.0022	.0012	____	____	4.02	18.02	4.02
1165	OSR	4	.042	0	0	.00058	.00063	.000098	.0027	.00048	4.05	18.05	4.05
1180	Star Sensor	4	.18	0	0	.0011	.0030	.011	.006	.0011	4.2	18.2	4.2
1190	Star Sensor	4	.072	0	0	.0027	.0056	.0093	.0029	.00084	4.1	18.1	4.1
1210	ABL	4	.00036	0	0	.00027	____	____	.0009	.00017	4.0	18.0	4.0
1145	Ring	4	.02	6	<1	.00049	.00068	.0012	.001	.00023	10.0	24.0	76.0
1146	Ring	4	.013	6	<1	.00022	.00026	.0013	.0015	.00037	10.0	24.0	76.0
1147	Ring	4	.015	6	<1	.00033	.00024	.0004	.0011	.0003	10.0	24.0	76.0
1148	Ring	4	____	0	0	.00052	.00062	.00053	.00076	.0092	4.01	18.01	4.01

† A First Flight Orbiter Would Result in 45Å During the In Bay-Doors Closed Period

* For a first flight Orbiter the outgassing return flux will be 21Å on surfaces 1110, 1153, 1145, 1146 and 1147 and 15Å on surfaces 1111 and 1113

** Return flux during deployment is less than one angstrom

- Off nominal, 4.5 hour in bay-doors closed period, could result in 18Å deposition on all DSP surfaces.

- Off nominal, 24 hour in bay-doors open, period could result in 72Å deposition on DSP critical surfaces facing out of the payload bay.

- A first flight, virgin Orbiter would increase the deposition by 41Å for the in bay-doors closed period.